

Sydney Paltra, Inan Bostanci, Kai Nagel

## The effect of mobility reductions on infection growth is quadratic in many cases

Open Access via institutional repository of Technische Universität Berlin

### Document type

Preprint | Submitted version

(i. e. version that has been submitted to a publisher for (peer) review; also known as: Author's Original Manuscript (AOM), Original manuscript, Preprint)

### Date of this version

16. February 2024

### This version is available at

<https://doi.org/10.14279/depositonce-17965>

### Citation details

Paltra, Sydney; Bostanci, Inan; Nagel, Kai (2024). The effect of mobility reductions on infection growth is quadratic in many cases, Technische Universität Berlin, preprint. <https://doi.org/10.14279/depositonce-17965>.

Submitted to journal *Scientific Reports* (E-ISSN: 2045-2322 ) on 16. February 2024

### Terms of use

© This work is licensed under a Creative Commons Attribution 4.0 International license:  
<https://creativecommons.org/licenses/by/4.0/>

# The effect of mobility reductions on infection growth is quadratic in many cases

Sydney Paltra<sup>\*1</sup>, Inan Bostanci<sup>2</sup>, and Kai Nagel<sup>1</sup>

<sup>1</sup>Technische Universität Berlin, FG Verkehrssystemplanung und Verkehrstelematik,  
10623 Berlin, Germany

<sup>2</sup>Zuse Institute Berlin, 14195 Berlin, Germany

## Abstract

Stay-at-home orders were introduced in many countries during the COVID-19 pandemic, limiting the time people spent outside their home and the attendance of gatherings. In this study, we argue from a theoretical model that in many cases the effect of such stay-at-home orders on incidence growth should be quadratic, and that this statement should also hold beyond COVID-19. That is, a reduction of the out-of-home duration to, say, 70% of its original value should reduce incidence growth and thus the effective R-value to  $70\% \cdot 70\% = 49\%$  of its original value. We then show that this hypothesis can be substantiated from data acquired during the COVID-19 pandemic by using a multiple regression model to fit a combination of the quadratic out-of-home duration and temperature to the COVID-19 growth multiplier. We finally demonstrate that many other models, when brought to the same scale, give similar reductions of the effective R-value, but that none of these models extend plausibly to an out-of-home duration of zero.

## 1 Introduction

### 1.1 Motivation

The COVID-19 pandemic confronted nations worldwide with a serious medical crisis, but also a cascade of economic, social, and psychological challenges. In this context, many countries implemented non-pharmaceutical interventions (NPIs, [1]) initially as part of a suppression strategy, but later as part of a risk mitigation strategy. Throughout the implementation of these NPIs, and particularly in the aftermath, significant efforts have been made to quantify their effectiveness and their interrelation with disease indicators, such as the effective  $R$ -value and hospitalization numbers.

For example, previous work work by [2] focuses on the first wave of the pandemic to link NPI introduction dates to national case and death counts. The authors find that school and university closures are most effective in reducing transmissions. However, their approach cannot distinguish direct effects on transmission within these institutions from potential indirect effects, such as changes in public behavior prompted by the signaling effect of school closures. Furthermore, they note that the disease burden may have been reduced by unobserved NPIs or voluntary behavior (e.g. mask wearing). Contrarily, in a follow-up study by the same group, [3], a significantly smaller effect size of the NPIs was observed during the second wave compared to the first. They attribute this decrease to differences in pre-intervention contact patterns, safety measures, personal protective behaviors, and the reduced adherence to NPIs. Notably, the impact of school closures was much smaller during the

---

\*correspondence: paltra@tu-berlin.de

second wave, possibly influenced by safety measures and behavioral changes (e.g., symptom screenings, asymptomatic testing, sanitizing) at schools. The authors speculate that the timing of school closures during the second wave, as they were now among the later NPIs, may have contributed to a reduced signaling effect.

Another example is the work by [4] that analyzed NPIs implemented in March–April 2020 across various countries. The study revealed that canceling small gatherings had the most significant impact on the effective R-value, followed by closing educational institutions. They find that for the closure of educational institutions and the cancellation of small gatherings, among many other NPIs, an early implementation is always more beneficial. The study concludes that NPI effectiveness is influenced by governance, epidemic stage, socio-economic factors, cultural and political characteristics, and previously implemented NPIs. Just like in the two aforementioned works, the authors of [4], directly translate NPIs to disease indicators and do not take into account the population’s time-dependent adherence.

We, however, inspired by [5–8], believe the population’s compliance to be a paramount intermediate step when quantifying NPIs’ effectiveness. Consequently, we decompose the effect of government-mandated NPIs into two steps:

1. Government-introduced NPIs influence the population’s behavior.
2. The population’s behavior influences the (effective) R-value/incidence growth.

In this work, we concentrate on the second step. That is, we do not discuss how strictly the population follows government-mandated behavior, and instead investigate how revealed behavior influences incidence growth. Here, the availability of mobility data from cellphones serves as a valuable proxy for revealed behavior, thus allowing investigations hitherto impossible. Indeed, many studies have stressed correlations and plausible causal connections between mobility and incidence growth; see Section 1.2.2 for details. In this paper, we go beyond these in the following way: First, we propose a theoretically motivated linear-in-parameters regression model, which we test with empirical data. Then, we translate models from related work into our proposed model and show thereby that the effect size we found is consistent with the literature.

One important outcome of our investigations is that the effect of mobility reductions in many situations is *quadratic*. That is, a reduction of the population mobility to, say, 70% of its normal value leads to a reduction of incidence growth to  $70\% \times 70\% = 49\%$  of its original value.

We begin by reviewing the currently existing literature, presenting alternative models and their results on the impact of mobility on disease spread. In the results section, we first investigate multiple mobility-only models, settling on the quadratic no-intercept version, before arguing for the inclusion of a temperature-related variable and deriving our final regression model. We then discuss the implications of the chosen model, and in particular compare it to other models. Finally, in the methods section we present an exploratory analysis of the included variables as well as a more detailed description of the model building process.

## 1.2 Literature Review

### 1.2.1 Relationship between COVID-19 and mobility in Germany

Multiple studies investigate the reduction of mobility in Germany related to the COVID-19 pandemic. None of these studies quantitatively investigates the consequences of these reductions for the infection dynamics. For more information on these studies, see Supplementary section 5.1.

### 1.2.2 Relationship between COVID-19 and mobility world-wide

Taking on a global perspective, we discuss studies which quantify the influence of mobility reductions on the infection dynamics. For the first four models described in the following, we have been able to

reconstruct the full model. Thus, we present them in more detail and compare them to our model in Section 4.4.

[9] use mobility data as a proxy measure for social distancing to characterize the relationship between transmission and mobility for 52 countries during the first year of the pandemic. They split the year into two country-specific periods, estimating for each period the log of the effective reproduction number as a function of the log of the basic reproduction number and a mobility indicator. The authors compute an adjusted  $R^2$  of 0.94 for the 1st period (before the change of the relationship occurred) and an adjusted  $R^2$  of 0.45 for the second period (after the change of the relationship occurred).

Considering a similar time frame and using the mobility indicators from the Google mobility reports for 125 countries as well as 52 US states/regions, [10] analyze the correlation between effective reproduction number and mobility. Using Pearson correlation test and linear modeling, the authors identify countries for which the correlation between  $R_t$  and mobility indicators was either a) negative, b) positive, or c) more complex than a linear relationship. In case of c), they additionally presented a quadratic model to improve their results.

[11] uses a fixed-effects model that controls for state-level effects to explore the relationship between Google mobility data and  $R_t$  (considering a 7-day and 14-day lag) on US state level, finding a positive correlation for retail/recreational activity and public transit, smaller association for shopping at grocery stores and pharmacies, and negative coefficients for time spent in residential areas.

Concentrating on five public health units (PHU) in the Greater Toronto Area in Canada and with the help of segmented regression, [12] assess the relationship between the effective R-value  $R_t$  and each Google mobility variable separately. They find a more pronounced relationship during the first wave than during the second wave in Canada.

Using mobile phone data from Teralytics, [13] demonstrate how the relative change in mobility (as a proxy for social distancing) correlates with the rate of new infections in the 25 US counties that had the highest number of confirmed cases on April 26, 2020. The authors fit a generalized linear model for each county, using a generalized Covid-19 growth rate, defined as the logarithm of the average number of new cases over the previous 3 days divided by the logarithm of the average number of new cases over the previous 7 days. The large divergence between this approach and the methodology proposed in this paper does not allow for a meaningful comparison, and is therefore omitted from our discussion in Section 2.5.

Finally, [14], [15], [16], [17], [18], and [19] find correlations between mobility and COVID-19 indicators, but do not present coefficients: [14] present a simple statistical model using mobility data, day-of-week variables, and indicators for changes in testing regimes that allows the generation of a 10-day forecast for 80 countries. [16] find that travel between US counties decreased by up to 35% during the first wave, but recovered rapidly during the partial reopening phase, and [15] showed with the help of an SEIRL (where L stands for isoLated) model that initial lockdowns and mobility suppressed the first COVID-19 wave in 12 global regions. Focusing on data from the first year of the pandemic, [19] relate all Google mobility categories apart from “residential” to new daily confirmed cases, finding that different kinds of community mobility were significant predictors of COVID-19, while [18] relate population, temperature, mask compliance, and the first principal component of Google’s six mobility variables to the log of the weekly infection growth rate and identify considerable spatiotemporal variations. Considering the first Omicron surge in the US, [17] use principal component analysis to relate Google mobility to COVID-19 case incidences in US counties, finding the coefficient of the “residential” mobility category to be the second largest in magnitude and the only one that is negative (PCA coefficient =  $-0.4571$ ).

### 1.3 Relating mobility to the growth multiplier

In our previous work [20], we discuss how the reduction of participation has a *quadratic* effect for gatherings. Work by [21], which focuses on the special case of in-person work meetings, comes to the same conclusion: If only a fraction  $\alpha < 1$  of a base turnout is present, then only that fraction  $\alpha$  can bring the infection to the gathering, just as only a fraction  $\alpha$  can become infected. In consequence, the base number of infections is multiplied by  $\alpha \cdot \alpha = \alpha^2$  under such circumstances. More precisely,

for a gathering of  $N$  persons, where  $p_{contag}$  denotes the probability to be contagious,  $p_{contag} \cdot N$  is the expected number of contagious attendees. On the other hand, when  $p_{inf}$  denotes the probability to get infected (conditional on being in the same room with an infected person), then the expected number of attendees who get infected per contagious person is  $p_{inf} \cdot (N - p_{contag} \cdot N)$ , i.e. the overall expected number of infected persons is

$$I_{fullTurnout} = p_{contag} \cdot N \cdot p_{inf} \cdot (N - p_{contag} \cdot N) .$$

If the turnout is reduced by multiplying it with a factor  $\alpha < 1$ , the expected number of infections is reduced to

$$p_{contag} \cdot \alpha N \cdot p_{inf} \cdot (\alpha N - p_{contag} \cdot \alpha N) = \alpha^2 \cdot (p_{contag} \cdot N \cdot p_{inf} \cdot (N - p_{contag} \cdot N)) = \alpha^2 \cdot I_{fullTurnout} .$$

The effect is quadratic only if all activity types (e.g. leisure, school, work) are reduced equally. Assume, for example, a situation in which only two out-of-home activities A and B are available, which have exactly the same characteristics (e.g. contact intensity, room size, indoor/outdoor activity, duration). Reducing participation at both to 50% yields a reduction of the out-of-home duration by half and a quadratic reduction of infections to  $50\% \cdot 50\% = 25\%$ . Conversely, completely shutting down activity A while leaving activity B completely open, only reduces infections by 50%, while still having the same reduction of the out-of-home duration.

In consequence, both linear and quadratic dependences of the growth multiplier on out-of-home duration are consistent with theory, making the type of relationship dependent on a country's handling of the pandemic. Furthermore, even higher order terms could be possible when the reduction of the out-of-home duration correlates with other infection-suppressing behaviors such as mask compliance or deliberately moving gatherings outdoors despite cold weather. In this case, we would observe the effect of reduced out-of-home duration, multiplied with the additional effects for which out-of-home duration would be a proxy.

## 2 Results

In this section, we present our findings on how mobility affects disease spread: Our model comparison confirms that mobility's influence in Germany was indeed quadratic. Moreover, including a weather variable improves the result, but mobility has a stronger influence than weather. Notably, weather only shows an effect in models that include mobility, underscoring the intricate interplay between these variables in shaping disease transmission dynamics.

### 2.1 Mobility vs. weather

The left panel of Figure 1 implies a correlation between out-of-home duration  $\mathbf{D}$  and the growth multiplier, defined as  $G_t = I_{t+1}/I_t$ , where  $I$  is the incidence of new cases and the index  $t$  numbers the weeks (for details on variables see Section 4.2). In contrast, there is no obvious correlation between the outdoor fraction and the growth multiplier (Figure 1, right panel), where the outdoor fraction is a transformation of the temperature taking into account that for very low and very high temperatures there needs to be saturation of the influence of weather; again see Section 4.2 for details. We thus start with a model based on the out-of-home duration before introducing the outdoor fraction. Because of the time lag between exposition to the virus and the reporting of cases, we employ a lead of 2.5 weeks on the reported case numbers; for details see Methods Sections 4.1 and 4.4.

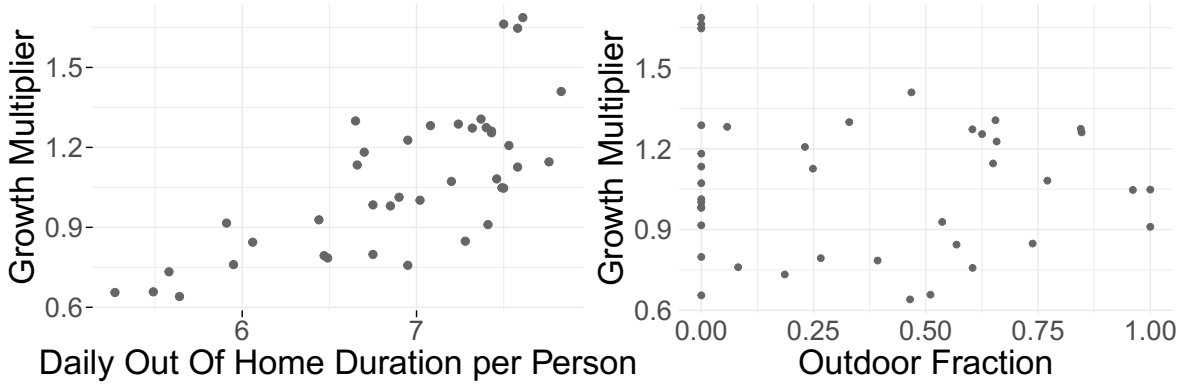


Figure 1: Left: growth multiplier  $\mathbf{G}$  vs. out-of-home duration (in hours)  $\mathbf{D}$ . Note that a base out-of-home duration of approximately 8 hours corresponds to a growth multiplier of around 1.5. Right: growth multiplier  $\mathbf{G}$  vs. outdoor fraction  $\mathbf{outFrac}$ . Growth multiplier lags behind out-of-home duration and outdoor fraction by 2.5 weeks.

## 2.2 Mobility only models

We now compare multiple mobility only models to establish if the influence of mobility on disease spread is linear, quadratic or cubic:

$$\mathbf{G}_{t+2} = \beta_0 + \beta_d \mathbf{D}_t, \quad (1)$$

$$\mathbf{G}_{t+2} = \beta_0 + \beta_{d^2} \mathbf{D}_t^2, \quad (2)$$

$$\mathbf{G}_{t+2} = \beta_0 + \beta_{d^3} \mathbf{D}_t^3, \quad (3)$$

where  $\mathbf{D}$  is the out-of-home duration in hours. The coefficients, which are computed using ordinary least squares, and summary statistics can be found in Table 1: The three models show similar values for  $R^2$ , the Akaike Information Criterion (AIC), and the Bayesian Information Criterion (BIC), and cannot be differentiated on these criteria alone.

Model	Adj. $R^2$	AIC	BIC	Variable	Coefficient	Std. Error	p >  t
Linear (1)	0.5207	-16.45	-11.38	Intercept	-0.9384	0.3068	0.0041
				$\mathbf{D}$	0.2910	0.0442	$8.98e - 08$
Quadratic (2)	0.5374	-16.82	-11.75	Intercept	0.0105	0.1626	0.949
				$\mathbf{D}^2$	0.0220	0.0033	$7.49e - 08$
Cubic (3)	0.527	-16.97	-11.90	Intercept	0.3278	0.1156	0.0073
				$\mathbf{D}^3$	0.0022	0.0003	$6.97e - 08$
Quadratic w/o intercept (4)	0.525	-18.82	-15.44	Intercept	0	n/a	n/a
				$\mathbf{D}^2$	0.0022	0.0006	$< 2e - 16$
Logarithmic (5)	0.589	-27.41	-22.34	Intercept	-3.6366	0.4881	$6.09e-09$
				$\log(\mathbf{D})$	1.9064	0.2528	$4.61e - 09$

Table 1: Regression output for different model types: linear, quadratic, cubic, quadratic without intercept, and logarithmic. The out-of-home duration  $\mathbf{D}$  leads by 2.5 weeks.

In this situation, theory, argues for (2): For an out-of-home duration  $\mathbf{D}$  close to zero, meaning that persons spend little time outside their own home, we would expect almost no disease spread, or in other words, a growth multiplier close to zero. According to Table 1, only the quadratic model has an intercept not significantly different from zero. The underlying reason for models (1) and (3) to compute an intercept significantly different from zero is that data on out-of-home duration  $\mathbf{D}$  during the pandemic in Germany ranges only from 5 to 9 hours per day (see Figure 2). Hence, a linear model would need to start from an intercept of almost  $-1$  to account for the relatively large slope of the data points within the observed range. Likewise, a cubic model would necessitate an intercept above zero to avoid an overly steep slope within the observed range.

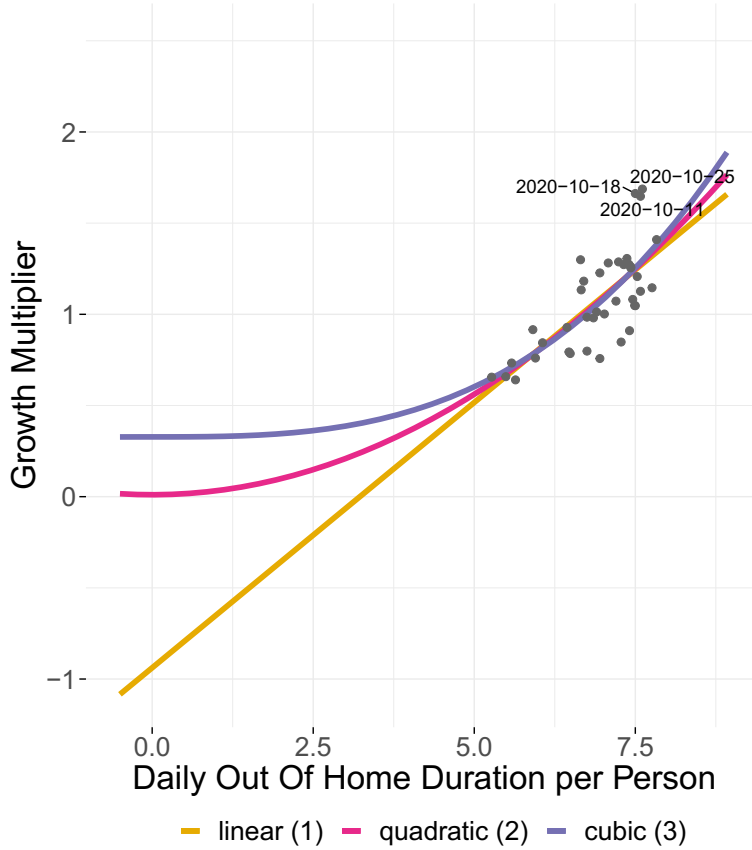


Figure 2: Growth multiplier vs. (average) daily out-of-home duration per person (in hours). Depicted are the regression lines of the linear (1), quadratic (2), and cubic (3) model.

Estimating the quadratic model (2) without the intercept, after inserting the estimated values (cf. Table 1), leads to

$$\mathbf{G}_{t+2} = 0.022 \cdot \mathbf{D}_t^2 . \quad (4)$$

To further confirm an exponent of 2, we estimate the exponent rather than just testing it for various integer values. We undertake this with linear regression by log-transforming the equation

$$\mathbf{G}_{t+2} = \gamma_0 \mathbf{D}_t^{\gamma_d} \quad (5)$$

$$\begin{aligned} \Leftrightarrow \log(\mathbf{G}_{t+2}) &= \log(\gamma_0) + \gamma_d \log(\mathbf{D}_t) \\ &= \tilde{\gamma}_0 + \gamma_d \log(\mathbf{D}_t), \end{aligned} \quad (6)$$

where we introduce  $\tilde{\gamma}_0 := \log(\gamma_0)$ . The regression output of (6) can be found in Table 1. Translated back into (5), this means

$$\mathbf{G}_{t+2} = 0.0263 \cdot \mathbf{D}_t^{1.9064} . \quad (7)$$

This is consistent with the quadratic model (4). In consequence, we continue with the quadratic no-intercept model.

### 2.3 Models including outdoor fraction

Using mobility alone, we are able to explain more than half of the variance in the growth multiplier. It is well known that seasonality also influences COVID-19's infection dynamics [22–24]. There are multiple mechanisms that may play a role, including that the stability of the virus may depend on ambient temperature, ambient humidity, or UV radiation, which is higher during summer. In our prior

research [20], we introduce the concept of an “outdoor fraction” (see Section 4.2 for its derivation). Here, we explore incorporating the outdoor fraction **outFrac** in addition to and as a cross term with mobility into our analysis. This yields

$$\mathbf{G}_{t+2} = \beta_{d^2} \mathbf{D}_t^2 + \beta_o \mathbf{outFrac}_t + \beta_{od^2} \mathbf{D}_t^2 \cdot \mathbf{outFrac}_t. \quad (8)$$

The regression output is given in Table 2.

Model	Adj. R <sup>2</sup>	AIC	BIC	Variable	Coefficient	Std. Error	p >  t
(8)	0.6345	-25.2865	-18.5310	<b>D</b> <sup>2</sup>	0.0242	0.0008	< 2e - 16
				<b>outFrac</b>	0.0167	0.3976	0.967
				<b>D</b> <sup>2</sup> · <b>outFrac</b>	-0.0053	0.0074	0.478
(9)	0.6345	-27.2846	-22.2180	<b>D</b> <sup>2</sup>	0.0242	0.0008	< 2e - 16
				<b>D</b> <sup>2</sup> · <b>outFrac</b>	-0.0050	0.0015	0.0017

Table 2: Regression output for different modes including the outdoors fraction. The out-of-home duration **D** leads by 2.5 weeks.

Two reasons speak against including the linear term **outFrac**. The first reason is a statistical one: Its coefficient is not significant and displays the highest p-value (see Table 2). The second reason is based on theory: Without mobility, the outdoor fraction has little to no influence on the infection dynamics. If a primary case is brought into a household, which spends all its time inside, then the whole household may become infected. But, if the household isolates itself, then no secondary cases outside the household will occur and the primary case will not influence society’s growth multiplier. Consequently, **outFrac** is dropped and we consider the model

$$\mathbf{G}_{t+2} = \beta_{d^2} \mathbf{D}_t^2 + \beta_{od^2} \mathbf{D}_t^2 \cdot \mathbf{outFrac}_t, \quad (9)$$

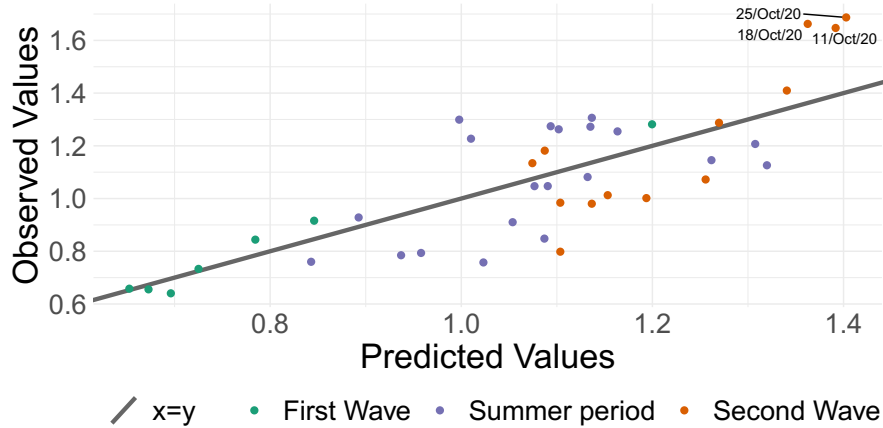
for which Table 2 shows the estimation results, with no discernible loss in explanatory power, improved AIC and BIC, and now all coefficients significant. With this, the overall mobility effect of 0.022 from Model (4) is split into a base positive effect of 0.024 and a negative effect of -0.005 stemming from the interaction of mobility and the outdoor fraction:

$$\begin{aligned} \mathbf{G}_{t+2} &= 0.024 \cdot \mathbf{D}_t^2 - 0.0050 \cdot \mathbf{D}_t^2 \cdot \mathbf{outFrac}_t \\ &= (0.024 - 0.0050 \cdot \mathbf{outFrac}_t) \cdot \mathbf{D}_t^2. \end{aligned} \quad (10)$$

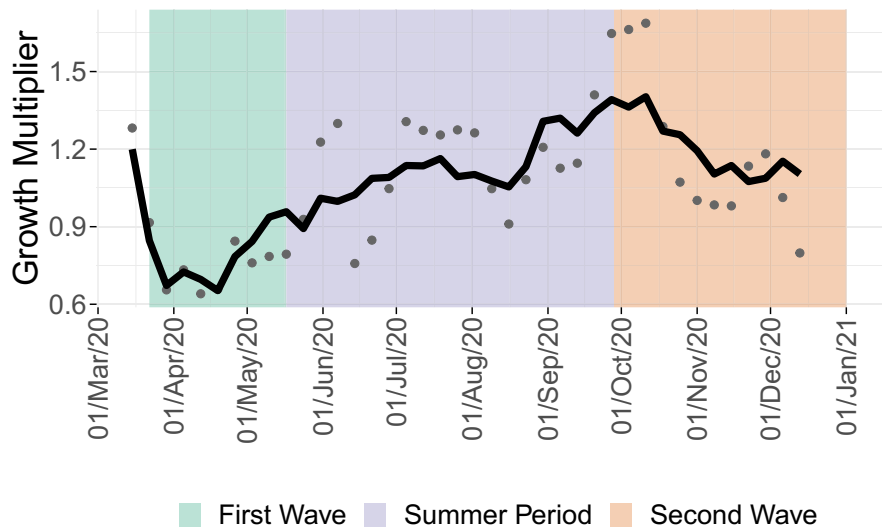
## 2.4 Final model

The model (10) is supported by theory, and it also displays the best fit of all models considered so far. In Section 5.3 (supplementary material), we consider an exhaustive comparison between model variations with terms up to the third degree, and arrive at the same result. We therefore keep (10) as our final model and inspect it further in this section.

Figure 3a displays the predicted vs. the observed growth multiplier in different colors for the first wave, the summer period, and the second wave for the final model (10). From the figure, we infer that the final model (10) is able to fit the data well. During the first wave, apart from the earliest data point, the observed as well as the predicted values are smaller than 1 – the reason is that the lagged growth data starts at the end of March, when the peak of the first wave had almost been reached (see Figure 6). Then, over the summer, the observed values display strong fluctuations, taking on values between  $\sim 0.75$  and  $\sim 1.35$ , where our fit predicts values closer to 1. This is consistent with a low incidence situation, where the “true” value is actually close to one, but random effects cause strong relative fluctuations. During the second wave, the three largest values are observed (see top-right corner of the plot) but the model underestimates the infection growth. Figure 3b displays the observed and the predicted growth rate over time. The plot over time again underlines one shortcoming of the least squares method: When strong relative fluctuations are encountered (such as during the summer period), then the linear fit will predict the average over those fluctuations.



(a) Observed growth multipliers vs. predicted growth multipliers.



(b) Growth multiplier over the course of 2020. Dots represent the observed, the line the predicted values.

Figure 3: Top: Observed growth multipliers vs. predicted growth multipliers. Bottom: Growth multiplier over the course of 2020. Dots represent the observed, the line the predicted values.

Overall, our model (10) is supported by theoretical considerations and has a good model fit. It is plausible that some of the variance that is not explained by our model, especially during the summer period, is stochastic, and thus cannot be explained by our type of model. A remaining issue are the three data points in October 2020, where the growth multiplier is larger than predicted by our model for three consecutive weeks, indicating that there must have been mechanisms in play that are *not* captured by our model.

## 2.5 Comparison of Our Model to Models in the Literature

Our model results may be compared to values from the literature for some but not all of the models introduced in Section 1.2.2. For some models a comparison is not possible as they report the quality of the fit but omit information necessary to reconstruct the full model. For other models the slope is reported, but not the intercept (models by [11] and [12]). In these cases, we use the base R-value of our model,  $R_{0,winter} = 1.4$ , but point out that this limits the comparability. Finally, for some of the models all necessary coefficients are available, thus allowing comparison to our model (models by [9] and [10]).

To compare the influence of mobility reduction across models, we choose the exemplary scenario in which the out-of-home duration is decreased by 40%. For the detailed comparison to each of the models [9–12] see Methods Section 4.4. The model comparison yields three findings:

Model	[9]	[10]	[11]	[12]	Our model (9)
$\Delta R$	-0.44	-0.42	-0.53	[-0.7, -0.36]	[-0.75, -0.6]
$R_t$ at $\mathbf{D} = 0$	0.21	0.1	0.43	-0.35	0

Table 3: Comparison of reduction of the effective R-value  $\Delta R$  when we assume a reduction of the out-of-home duration by 40% across models and comparison of the resulting R-values when we assume an out-of-home duration of 0. [9] provide  $R_{0,i} = 0.97$ , allowing us to compute  $R_t$  at  $\mathbf{D} = 0$ . In [10] a plot of the regression line can be found in the supplementary material. We computed  $R_t$  at  $\mathbf{D} = 0$  after reading the intercept from the plot and again under the assumption that the average at-home duration is 16 hours. [11] and [12] do not provide a value for the intercept. Consequently, in these cases we base the computation of the effective R-value if the out-of-home duration  $\mathbf{D}$  is equal to zero (second line) on our  $R_{0,winter} = 1.4$  of (11).

First, all models, including our own, find a reduction of the effective R-value between  $-0.36$  and  $-0.75$  if the daily out-of-home duration is reduced by 40% or 3.2 hours (see Table 4). This, by itself, already implies a remarkable consistency across the different locations and models. Figure 4 displays the five different regression curves, and we note that to fit our data cloud, a linear slope, as used in the models by [10] and [12], suffices.

Second, we note that when extrapolating the fit to an out-of-home duration of zero, some form of curvature is necessary to meet the requirement that the R-value is equal to zero when the mobility is zero. Without curvature, one either needs an intercept significantly below zero (grey line in Figure 4, or the slope is not steep enough to be consistent with the data points (yellow line in Figure 4; see also Figure 2). – For the curved models by [9] (green curve) and [11] (brown curve), it is unclear if they could be adapted such that they both have the correct slope through the data *and* go through the origin.

Overall, this implies that these models are valid in the range of values where they are estimated, but do not extrapolate well beyond that range. In contrast, our quadratic model computes a growth multiplier (and thus R-value) of zero when the out-of-home duration is zero and thus allows for plausible extension to the case when the mobility is zero.

Third and last, we point out that the preceding two arguments are consistent with Section 2.2 and especially Figure 2, in which we already argue for a quadratic relationship between time spent outside one’s home and the growth multiplier/R-value.

In conclusion, our own model goes beyond the existing models, since we start from a hypothesis about the underlying mechanism, and from there develop a theory (see Section 2.2). In consequence, our model is easier to adapt to changing circumstances.

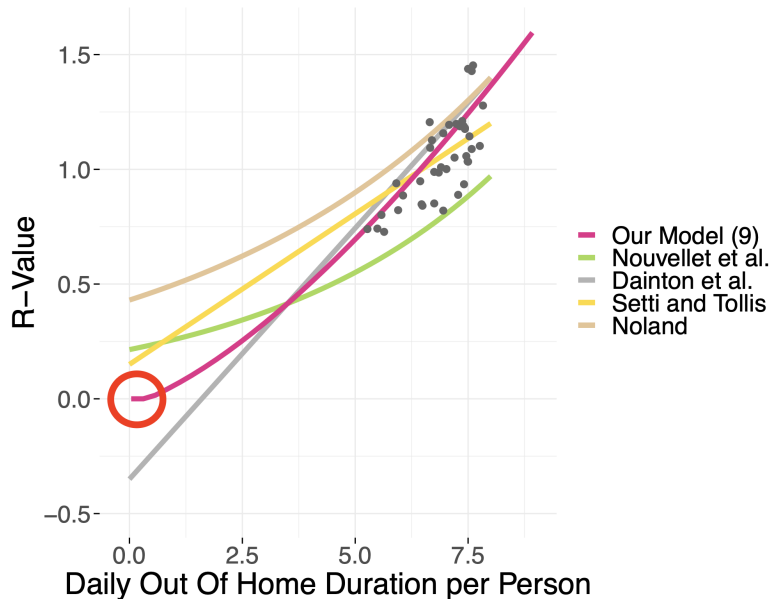


Figure 4: R-value vs. average daily out-of-home duration per person (in hours). Depicted are our quadratic model (9), the models by Nouvellet et al. [9], Setti and Tollis [10], Noland [11], and Dainton et al. [12]. For our model, the growth multiplier was converted to the R-value, while for the models by [9], [10], [11], and [12], the percentage change in mobility was converted to the absolute out-of-home duration (in hours). For [11] and [12], as no intercept is provided, we used  $R_{0,winter} = 1.4$  of (11), which implies that the actual regression lines by [11, 12] are potentially shifts of our depictions. The red circle marks the origin, through which all models should plausibly go.

## 2.6 Consequences for Disease Management and Extension to Other Communicable Diseases

A quadratic reduction of the number of infections as a consequence of mobility reductions is most consistent with the data. This is also consistent with the theory developed in Section 1.3, which states that, if the base turnout at a gathering is reduced to a fraction  $\alpha < 1$ , then both the contagious and susceptible fractions are reduced, leading to a reduction of infections to  $\alpha \cdot \alpha < \alpha$ . One question that arises is if this is related to the disease transmission mechanism. Section 1.3 has already pointed out that the result would be different if activity types were not reduced equally, but selectively. Similarly, the result would be different if the number of susceptible persons with which contagious persons interact would not be reduced – then the reduction factor of  $\alpha$  would no longer apply to the susceptibles. For COVID-19, a possible scenario for this would be a workplace where, for a turnout of  $\alpha$ , also a fraction  $1 - \alpha$  of the available offices would no longer be used, crowding the remaining employees in only  $\alpha$  of the office space. In that situation, the number of contagious persons would be reduced by  $\alpha$ , but the number of persons each of them encounters would be the same as before. A similar situation exists with schools: If the turnout for each class is reduced to  $\alpha = 0.5$ , then the number of infections is reduced to  $0.5 \cdot 0.5 = 0.25$ . If, however, a scheme of “alternating classes” is used (as was done in Germany, see for example [25]), then the situation is similar to the offices above since half of the classrooms are no longer used, and in the other half of classrooms, the reduced number of contagious persons interacts with the same number of susceptible persons as without the “alternating classes” intervention.

This line of thinking extends to different transmission mechanisms: For aerosol transmission, to first order one may assume that every susceptible person in the room obtains the same dose (since breathed-out aerosols have a tendency to first rise to the ceiling and from there distribute through the room [26, 27]). For droplet infection, one may assume that only persons in close distance can become infected – here, only if the number of susceptible persons within close distance is also reduced by  $\alpha$ , the quadratic relationship holds. As a rule of thumb, reducing person densities will lead to the quadratic reduction, whereas fully shutting down activities while maintaining others at the same person densities as before will lead to an only linear reduction – and this is expected to be largely independent from the exact mechanism of disease transmission.

### 3 Discussion

Using a multiple linear regression model, we look into how mobility, temperature, and the COVID-19 growth multiplier are related. We find that more than 50% of the variance of the growth multiplier can be explained by the out-of-home duration alone. Furthermore, for most data sets, including our own, the elasticity of the growth multiplier with respect to changes of the out-of-home duration is larger than one. This means that a linear fit of such data points extrapolates, for out-of-home durations of zero, to negative growth multipliers – which is not plausible. In contrast, a quadratic model fits the data well, generates a growth multiplier of zero at out-of-home durations of zero, and can be motivated by theory.

Temperature alone was a worse predictor of the growth multiplier than the out-of-home duration. Temperature does provide, however, a good correction to the out-of-home duration, leading to a regression that explains more than 60% of the variance of the growth multiplier.

The growth multiplier follows changes in mobility with a delay of about 2.5 weeks. As there is only a 5-day period from infection to showing symptoms, this is longer than expected. A plausible explanation is that the German reporting system added considerable delay.

In this work, we use the growth multiplier  $G$  instead of the more well-known effective  $R$ -value as our response variable. This is motivated by the fact that for the effective  $R$ -value we would have to use external estimates (for example, see [28] and [29]), while the growth multiplier can be directly inferred from the readily available incidence data. We have computed a base growth multiplier of  $G_0 = 1.54$ , which translates to a base reproduction value of  $R_0 \approx 1.4$  (see Section 2.5). In the literature, the base reproduction number  $R_0$  for COVID-19 ranges between 1.5 and 3 [30], [31]. Although some authors argue that these estimations need to be adjusted for the increase in RT-PCR tests [32], our value is on the lower end of what can be found in the literature. A possible reason for this is that there may be additional effects, such as people being careful, people wearing masks, etc., which may have remained in place during summer 2020 even during phases of large mobility.

In general, our proposed linear-in-parameters regression model performs well. Much of the remaining variance not explained by the model can be credited to random fluctuations due to small numbers during low incidence phase. However, the model has systematic problems in the middle of October 2020: Figures 3a and Figures 3b show that our model underestimates the observed growth multiplier for three successive weeks in October, that is, mobility and temperature do not suffice to predict the sharp increase in case numbers. It appears that an additional mechanism, not accounted for by our model, is at play.

To this end, we explored if **school holidays** were responsible for the sharp increase. In Germany, the duration and time of school holidays depends on the federal state. In 2020, twelve out of sixteen federal states closed their schools for two weeks in fall, with Hamburg, Hesse, and Schleswig-Holstein starting on 05/Oct, Berlin, Brandenburg, Bremen, Lower Saxony, North Rhine-Westphalia, Rhineland-Palatinate, Saarland starting on 12/Oct, and Saxony and Thuringia on 19/Oct. The remaining four states only closed their schools for a single week: Mecklenburg-Vorpommern starting on 05/Oct, Saxony-Anhalt on 19/Oct and Baden-Württemberg and Bavaria starting on 26/Oct and 2/Nov respectively. Because of the time lag between exposition to the virus and the reporting of cases, manifested in our time lag of 2.5, even a school closure as early as 5/Oct is too late to explain an increase of the growth multiplier in the week of 11/Oct. Also, in Germany school holidays typically led to a *reduction* of infections – not only because schools were removed as infection contexts, but also because many parents no longer went to work during school holidays.

Another possible influence might be **disease import** when returning from vacations. However, the earliest plausible time people could return in larger numbers is after the first week of school holidays, i.e. around 12/Oct. Clearly, this is again too late to have an influence on the growth multiplier in the week of 11/Oct.

Another factor to consider is **testing**. On 03/November/2020, the testing criteria in Germany were adapted. In consequence, the number of tests of 1.602.839 in calendar week 45 dropped to 1.390.324 in calendar week 46, and the German federal health agency RKI states that the testing numbers before and after the adaptation cannot be directly compared [33]. We acknowledge that this may influence

our fit for the final weeks of 2020, but because of the time discrepancy reject adapted testing policies as the reason for the described underfit during the beginning of the fall wave.

We also explored if a **sudden temperature** drop at the end of August (see Fig. 8) might have led to people moving their activities indoors despite higher temperatures at the end of September. In fact, the Google mobility data [34] shows that the visits to parks sharply declined in mid-September and did not increase again within the study period. In consequence, we modified the outdoor fraction such that it would never *increase* during fall 2020 – i.e. once people had decided to move a certain fraction of activities indoors, they would not be moved outdoors again until the following spring. However, this did not significantly improve the fit of our model. Overall, we do not want to rule out that indoors/outdoors behavior might have played a role here. However, neither temperature nor park usage is sufficient to explain our three sequential outliers in October 2022.

## 4 Methods

### 4.1 Time scale and lag

We consider data for the first year of the pandemic, ranging from March 15, 2020 until December 13, 2020. Because the incidence in Germany was fluctuating strongly in February and early March 2020 due to small numbers and issues with the reporting system, February 2020 is excluded. As the German government announced stricter measures on Dec 13, 2020, which were installed on Dec 16, 2020 [35], the mobility data between December 13 and December 16 was heavily influenced by this announcement. Furthermore, testing and reporting during Christmas was delayed and unreliable, leading us to the exclusion of mobility data from December 13, 2020 onwards. Time is given in weeks, where  $t = 1$  corresponds to “15/Mar/2020” and the maximum  $t = 40$  corresponds to “13/Dec/2020”. Since the growth rate is defined as  $G_t = I_{t+1}/I_t$  (see below), the considered lag effectively is 2 ½ weeks.

### 4.2 Variables

Our considered response variable is:

- $\mathbf{G}_t := \frac{I_{t+1}}{I_t}$ , the multiplicative growth rate, which describes the change of incidence from one week to another. Hereby,  $I_t$  is the average 7-day incidence per 100,000 at time  $t$ .

The considered explanatory variables are:

- $\mathbf{D}_t$ : “Out of home duration”, which serves as a mobility indicator. Denotes in hours how much time an average person spends daily outside their home during week  $t$ .
- $\mathbf{Tmax}_t$ : Weekly average of the daily maximum temperature (in Celsius), see Section 4.3.3 for details.
- $\mathbf{Tavg}_t$ : Weekly average of the daily average temperature (in Celsius), see Section 4.3.3 for details.
- $\mathbf{Precip}_t$ : Weekly average of daily total precipitation (in mm).
- $\mathbf{outFrac}_t$ : “Outdoor fraction”, a transformation of  $\mathbf{Tmax}_t$  following the example of [20] and computed in two steps:

This approach is motivated by the argument that, if the effect of the temperature is mostly transmitted via the indoors/outdoors behavior, it needs to saturate at the lower end because eventually all activities are indoors, and at the upper end because eventually all activities are outdoors. Such a behavior is typically modeled with an S-shaped function such as a logit function.

Those functions are characterized by a midpoint and a slope at that midpoint. Thus, first, we introduce a time-dependent midpoint  $T_t^*$  equal to

$$T_t^* = \begin{cases} 7.5/30 * t + 17.5 & \text{if } t \leq 30, \\ 25 & \text{if } t > 30. \end{cases}$$

In the second step, we then approximate said S-shaped function with a piecewise linear function with midpoint  $T_t^*$  (as defined above), and slope 0.1:

$$\text{outFrac}_t(\mathbf{Tmax}_t) = \begin{cases} 0 & \text{if } \mathbf{Tmax}_t < T_t^* - 5, \\ \frac{\mathbf{Tmax}_t - (T_t^* - 5)}{10} & \text{if } T_t^* - 5 \leq \mathbf{Tmax}_t \leq T_t^* + 5 \\ 1 & \text{if } \mathbf{Tmax}_t > T_t^* + 5, \end{cases}$$

where  $\mathbf{Tmax}_t$  denotes the weekly average maximum temperature (in Celsius).

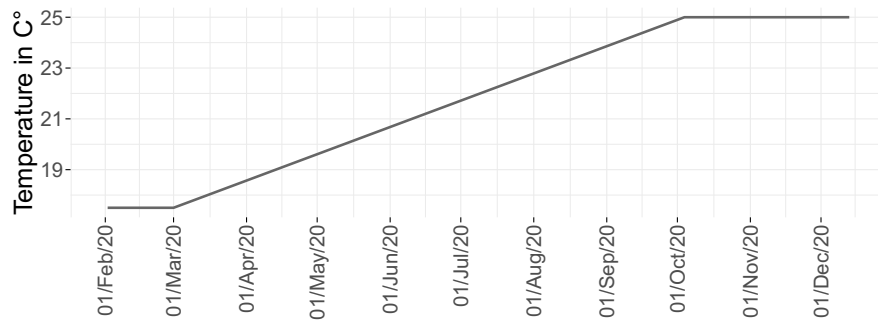


Figure 5:  $T^*$  over the course of 2020.

This approach is motivated by our modelling work in fall 2020, where a higher sensitivity to sinking temperatures after a warm summer was a plausible explanation for the timing of the beginning of the second wave [20]. Hence, at  $t = 1$  (corresponding to “15/March/2020”), people are willing to spend half of their time outside if  $T^* = 17.5$ . Over the course of the year, this threshold linearly increases until it reaches  $T^* = 25$  in the fall at  $t = 30$  (corresponding to “04/October/2020”).

## 4.3 Exploratory analysis

### 4.3.1 Growth multiplier

The top plot of Figure 6 shows the weekly average of the reported 7-day incidence/100,000 as provided by Robert-Koch-Institut (RKI) [36]. In Germany, the first COVID-19 wave began in calendar week 10 (starting 02/March/2020) and lasted until calendar week 20 (ending on 17/May/2020). It was followed by a summer period of low infection numbers, before the second wave began on 28/September/2020 [37]. The bottom plot depicts the multiplicative rate by which the COVID-19 case incidence changed from week to week (see Sec 4.2 for definition).

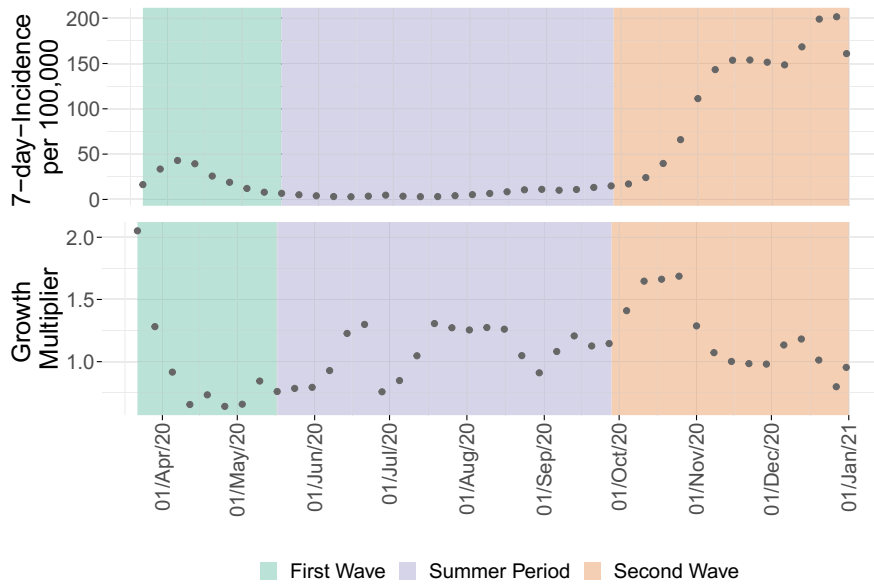


Figure 6: Top: 7-day-incidence/100,000 over the course of 2020. Bottom: Growth Multiplier for 2020.

### 4.3.2 Out Of Home Duration

Figure 7 depicts the amount of time (in hours) an average person spends outside their home per day. We note that when contact restrictions were introduced (23/March/2020), the out-of-home duration had already decreased and it reached its minimum in the week of the introduction of the contact restrictions. The out-of-home duration did not plateau at this minimum and in consequence, an increase can already be seen before the first NPIs were officially relaxed in calendar week 19/20 (beginning on 04/May/2020 and 11/May/2020 respectively) [38]. During the summer, out-of-home duration surpassed the pre-pandemic level of early March 2020, which is expected when comparing summer and early spring duration. Finally, starting in late September we see another decrease in out-of-home duration. The so-called “lockdown light”, which was introduced on 02/November/2020, lead to an additional local maximum (potentially due to hasty Christmas-shopping) before the introduction of more restrictive contact restrictions on 16/December/2020.

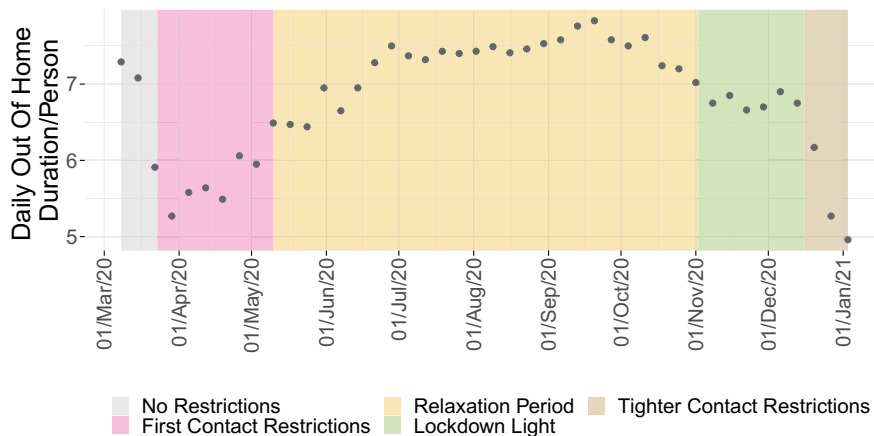


Figure 7: Daily out of home duration per person (in hours) for 2020.

### 4.3.3 Outdoor Fraction

The top plot of Fig. 8 depicts the maximum temperature (in  $C^\circ$ ) over the course of 2020. We first average over weeks, then over federal states. For the latter, we take the weekly average of the maximum temperature of every federal state’s capital. We then average over these 16 values, weighting values according to states’ population shares. Bottom plot: As explained in Section 4.2, we assume that there exists a season-dependent threshold below (or above) which the share of leisure activities performed inside (or outside) does not further decrease (or increase). In consequence, the maximum temperature is transformed to the so-called “share of activities performed outside”, or in short “outdoor fraction”.

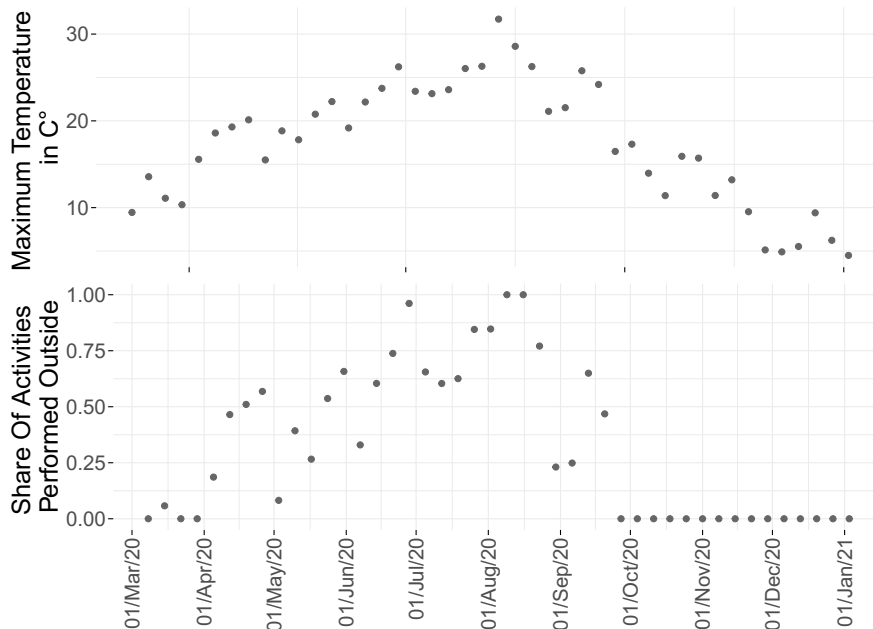


Figure 8: Top: Maximum temperature (in  $C^\circ$ ). Bottom: Share of leisure activities spent outside.

## 4.4 Model Comparison

To settle on the final model (9), we employ a multi-step model comparison:

- In the first step, we consider mobility-only models (see Section 2.2 for details), to determine if the influence of mobility on the growth multiplier was linear, quadratic or cubic.
- Then, we compare the intercept and no-intercept model arguing for the exclusion of the intercept (again, see Section 2.2).
- In the third step, we compare multiple weather variables: the weekly average of the daily maximum temperature **Tmax**, the weekly average of the daily average temperature **Tavg**, the weekly average of the daily total precipitation **Precip**, and the outdoor fraction **outFrac**. Model outputs and detailed discussion of this step can be found in the Supplementary Material 5.3.
- In the final step, we exclude the linear term for **outFrac** and only include the interaction term of out-of-home duration and **outFrac** (see Section 2.3).

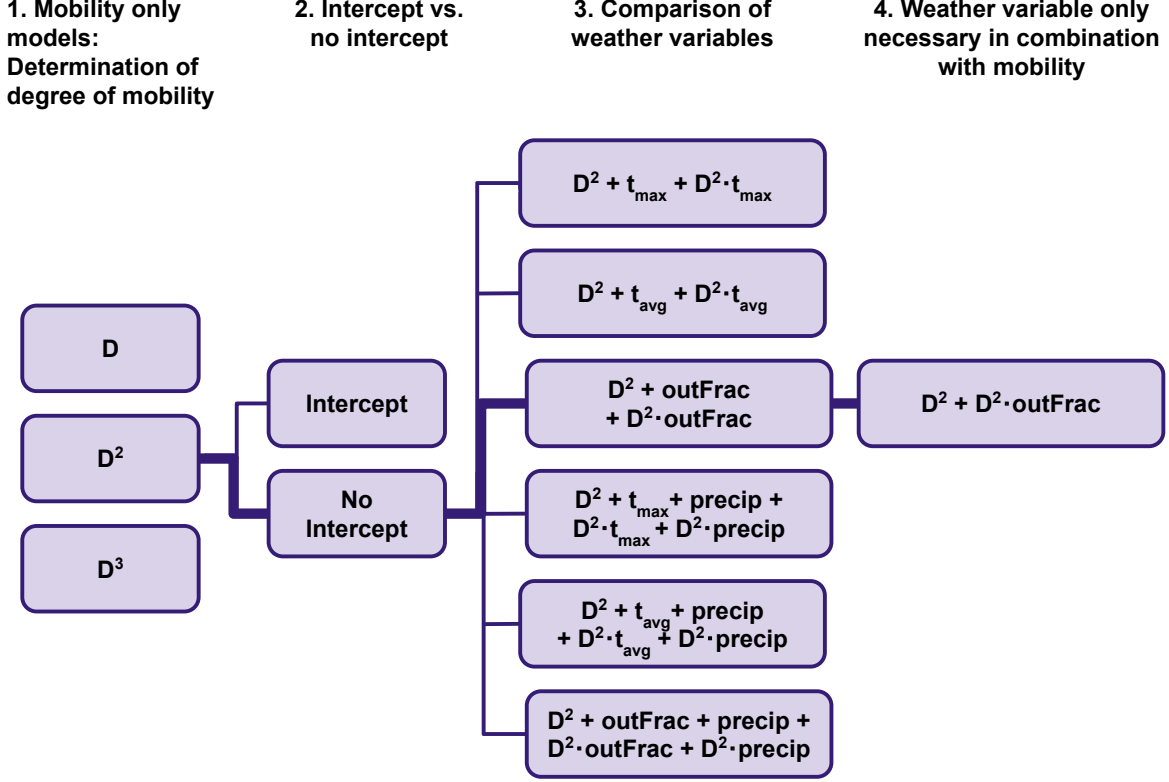


Figure 9: Multi-step model comparison to determine the final model (9).

## 4.5 Comparison of Our Model to Models in the Literature

As address in Section 2.5, we compare our model values to values in the literature whenever possible. This is not possible for the publications that report the quality of the fit but omit information necessary to reconstruct the full model (see Section 1.2.2). However, the following four papers provide the necessary coefficients and can thus be compared to our model.

To compare the influence of mobility reduction across models, we choose the following scenario: For all comparisons, we assume that the out-of-home duration is decreased by 40%. The average German out-of-home duration is around 8 hours per day (see Figure 10 and Supplementary Section 5.2), leading to an average *at-home* duration of about 16 hours per day. Reducing the out-of-home duration by  $-40\%$ , or  $-3.2 \text{ hrs}$ , to  $4.8 \text{ hrs}$  thus corresponds to increasing the *at-home*-duration by 20%.

According to (10), our base growth multiplier  $\mathbf{G}_{0,winter}$ , at  $\mathbf{D} = 8 \text{ hours}$  and  $\text{outFrac} = 0$ , is 1.54. In order to translate the weekly growth multiplier to the R-value, the generation time needs to be taken into account. Assuming the generation time of SARS-CoV-2 as 5 days [39–41], we obtain

$$R_{0,winter} = \mathbf{D}_{0,winter}^{5/7} = 1.54^{5/7} \approx 1.4 . \quad (11)$$

Assuming the aforementioned reduced out-of-home time of  $8 \text{ hrs} - 3.2 \text{ hrs} = 4.8 \text{ hrs}$ , we obtain

$$R_{winter}(-3.2 \text{ hrs}) = (\mathbf{D}_{winter}(-3.2 \text{ hrs}))^{5/7} = (0.024 \cdot 4.8^2)^{5/7} \approx 0.55^{5/7} \approx 0.65 . \quad (12)$$

The corresponding reduction of the effective R-value thus is

$$\Delta R_{winter} := R_{winter}(-3.2 \text{ hrs}) - R_{0,winter} \approx 0.65 - 1.4 = -0.75 . \quad (13)$$

The same computation, with  $\text{outFrac} = 1$ , i.e. “during summer”, leads to  $\Delta R_{summer} \approx -0.6$ .

Some of the models we compare with are linear, and for these models  $\Delta R$  can be obtained from the slope coefficient without having to determine the intercept. In the following, we thus compare with our  $\Delta R$ , which is between 0.6 (warm summer) and 0.75 (cold winter).

**Comparison with [9]** [9] use

$$\log(R_{t,i}) = \log(R_{0,i}) - \beta_i(1 - m_{t,i}), \quad (14)$$

where  $m_{t,i}$  denotes the remaining fraction of mobility compared to a baseline, expressed as a value between 0 and 1. The remaining mobility fraction  $m_{t,i}$  is based on various categories from Google [34] or Apple [42] mobility data. The percentage changes must then be divided by 100 to obtain  $m_{t,i}$ . When using a combination of google and apple mobility data, the authors obtain  $\beta_i = 1.51$  and  $R_{0,i} = 0.97$  for Germany during the period from late April to late October 2020. Using our introduced example, namely a reduction of the out-of-home duration of 40% ( $= 0.4$ ), we obtain

$$\begin{aligned} \log(R_{Ger}) &= \log(0.97) - 1.51 \cdot 0.4 \approx -0.634459 \\ &\Leftrightarrow R_{Ger} \approx 0.53 \\ &\Leftrightarrow \Delta R_{Ger} \approx 0.53 - 0.97 = -0.44 . \end{aligned}$$

This is somewhat smaller, but still consistent with our own range of  $[-0.75, -0.6]$ .

**Comparison with [10]** [10] analyze the correlation between effective reproduction number and mobility. For the “residential” category, this leads to

$$R_t = \beta_0 + \beta_r \cdot h_{t-\tau}, \quad (15)$$

where  $R_t$  denotes the effective reproduction number and  $h_t$  denotes the percentage change of time spent at home as introduced above. For a 14-day lag ( $\tau = 14$ ) they compute a coefficient of  $\beta_r = -0.021$  for Germany. Hence, for a 20% increase of the at-home duration, their model computes a reduction of the effective  $R$ -value by  $-0.021 \cdot 20 = -0.42$ . Again, this is somewhat smaller, but still consistent with our own range of  $[-0.75, -0.6]$ .

**Comparison with [11]** [11] uses a fixed-effects model that controls for state-level effects to explore the relationship between Google mobility data and  $R_t$  on US state level. For the “residential” category, the model reads

$$\log(R_{t,state}) = \beta_{0,state} + \beta_r \cdot h_{t-\tau} + \beta_d \cdot days_t , \quad (16)$$

where  $\beta_{0,state}$  denotes a state-specific intercept,  $h_t$  denotes the percentage change of the “residential” category, and  $days_t$  is a trend variable denoting the days since the start of the pandemic in the state. He obtains  $\beta_r = -0.0236$  and  $\beta_d = -0.0020$  when considering a 14-day lag ( $\tau = 14$ ) between mobility and the effective  $R$ -value. The values of  $\beta_{0,state}$  are not given in the paper; to compare with our example one can set  $h_{t-\tau}$  and  $days_t$  to zero and then use  $\beta_{0,state} = \log R_0 = \log(1.4)$ . For our example of increasing the at-home-duration, we have  $h_{t-\tau} = 20$ , and thus

$$\begin{aligned} \log(R_t) &= \log(1.4) - 0.0236 \cdot 20 \approx -0.13553 \\ &\Leftrightarrow R_t \approx 0.87 \\ &\Leftrightarrow \Delta R_t \approx 0.87 - 1.4 = -0.53 \end{aligned}$$

Again, this needs to be compared with our range of  $[-0.75, -0.6]$ .

The trend variable  $days$  leads to even smaller reductions over time, but after a year,  $days = 365$  even with  $h_{t-\tau} = 0$  leads to an  $R_t < 1$ , which is clearly not plausible. Indeed, the model was estimated against data until June 23rd, 2020, and it is plausible that the trend term, at least in part, rather captures the seasonal effect.

**Comparison with [12]** For the “residential” category, [12] obtain the following model:

$$R_t = \beta_0 + \beta_r \cdot h_{t-\tau},$$

where  $h$  denotes the percentage change of the “residential” category. For the 14-day lag ( $\tau = 14$ ) the coefficient differs between the considered five public health units in the Greater Toronto Area and takes on values between  $-0.035$  and  $-0.018$ . Consequently, this leads to a reduction of the  $R$ -value between  $-0.035 \cdot 20 = -0.7$  and  $-0.018 \cdot 20 = -0.36$ , which overlaps with our range of  $[-0.75, -0.6]$ .

## 4.6 Data availability

All data used in this study is publicly available:

- RKI (incidence data): The 7-day incidence/100,000 inhabitants in Germany is provided by the Robert-Koch-Institut [36].
- Meteostat (temperature data): Meteostat [43] provides weather data on a daily basis, which served as the basis for **Tmax** (and consequently **outFrac**), **Tavg** and **Precip**.
- Senozon and TU Berlin (mobility data): The weekly out of home duration is available on Zenodo [44].
- Google (alternative mobility data source): Usage of Google COVID-19 Community Mobility reports in the supplementary material [34]. Google stopped reporting new data on October 15, 2022, but all published data is still publicly available.

## 4.7 Code availability

All code used to produce the results is publicly available on GitHub.

## References

1. Mathieu, E., Ritchie, H., Rodés-Guirao, L., Appel, C., Giattino, C., Hasell, J., Macdonald, B., Dattani, S., Beltekian, D., Ortiz-Ospina, E. & Roser, M. Coronavirus Pandemic (COVID-19). *Our World in Data*. <https://ourworldindata.org/coronavirus> (2020).
2. Brauner, J. M., Mindermann, S., Sharma, M., Johnston, D., Salvatier, J., Gavenčiak, T., Stephenson, A. B., Leech, G., Altman, G., Mikulik, V., Norman, A. J., Monrad, J. T., Besiroglu, T., Ge, H., Hartwick, M. A., Teh, Y. W., Chindelevitch, L., Gal, Y. & Kulveit, J. Inferring the effectiveness of government interventions against COVID-19. *Science* **371** (Feb. 2021).
3. Sharma, M., Mindermann, S., Rogers-Smith, C., Leech, G., Snodin, B., Ahuja, J., Sandbrink, J. B., Monrad, J. T., Altman, G., Dhaliwal, G., Finnveden, L., Norman, A. J., Oehm, S. B., Sandkühler, J. F., Aitchison, L., Gavenčiak, T., Mellan, T., Kulveit, J., Chindelevitch, L., Flaxman, S., Gal, Y., Mishra, S., Bhatt, S. & Brauner, J. M. Understanding the effectiveness of government interventions against the resurgence of COVID-19 in Europe. *Nature Communications* **12** (Oct. 2021).
4. Haug, N., Geyrhofer, L., Londei, A., Dervic, E., Desvars-Larrive, A., Loreto, V., Piniór, B., Thurner, S. & Klimek, P. Ranking the effectiveness of worldwide COVID-19 government interventions. *Nature Human Behaviour* **4**, 1303–1312 (Nov. 2020).
5. Seale, H., Dyer, C. E. F., Abdi, I., Rahman, K. M., Sun, Y., Qureshi, M. O., Dowell-Day, A., Sward, J. & Islam, M. S. Improving the impact of non-pharmaceutical interventions during COVID-19: examining the factors that influence engagement and the impact on individuals. *BMC Infectious Diseases* **20** (Aug. 2020).
6. Dönges, P., Wagner, J., Contreras, S., Iftekhar, E. N., Bauer, S., Mohr, S. B., Dehning, J., Valdez, A. C., Kretzschmar, M., Mäs, M., Nagel, K. & Priesemann, V. Interplay Between Risk Perception, Behavior, and COVID-19 Spread. *Frontiers in Physics* **10** (Feb. 2022).
7. Petherick, A., Goldszmidt, R., Andrade, E. B., Furst, R., Hale, T., Pott, A. & Wood, A. A worldwide assessment of changes in adherence to COVID-19 protective behaviours and hypothesized pandemic fatigue. *Nature Human Behaviour* **5**, 1145–1160 (Aug. 2021).
8. Kacelnik, O. & Kacelnik, A. Behavioral risk compensation and the efficacy of nonpharmacological interventions. *Behavioural Public Policy* **6**, 1–12 (2022).

9. Nouvellet, P., Bhatia, S., Cori, A., Ainslie, K. E. C., Baguelin, M., Bhatt, S., Boonyasiri, A., Brazeau, N. F., Cattarino, L., Cooper, L. V., Coupland, H., Cucunuba, Z. M., Cuomo-Dannenburg, G., Dighe, A., Djaafara, B. A., Dorigatti, I., Eales, O. D., van Elsland, S. L., Nascimento, F. F., FitzJohn, R. G., Gaythorpe, K. A. M., Geidelberg, L., Green, W. D., Hamlet, A., Hauck, K., Hinsley, W., Imai, N., Jeffrey, B., Knock, E., Laydon, D. J., Lees, J. A., Mangal, T., Mellan, T. A., Nedjati-Gilani, G., Parag, K. V., Pons-Salort, M., Ragonnet-Cronin, M., Riley, S., Unwin, H. J. T., Verity, R., Vollmer, M. A. C., Volz, E., Walker, P. G. T., Walters, C. E., Wang, H., Watson, O. J., Whittaker, C., Whittles, L. K., Xi, X., Ferguson, N. M. & Donnelly, C. A. Reduction in mobility and COVID-19 transmission. *Nature Communications* **12** (Feb. 2021).
10. Setti, M. O. & Tollis, S. In-depth Correlation Analysis of SARS-CoV-2 Effective Reproduction Number and Mobility Patterns: Three Groups of Countries. *Journal of Preventive Medicine and Public Health* **55**, 134–143 (Mar. 2022).
11. Noland, R. B. Mobility and the effective reproduction rate of COVID-19. *Journal of Transport & Health* **20**. ISSN: 2214-1405 (2021).
12. Dainton, C. & Hay, A. Quantifying the relationship between lockdowns, mobility, and effective reproduction number (Rt) during the COVID-19 pandemic in the Greater Toronto Area. *BMC Public Health* **21** (Sept. 2021).
13. Badr, H. S., Du, H., Marshall, M., Dong, E., Squire, M. M. & Gardner, L. M. Association between mobility patterns and COVID-19 transmission in the USA: a mathematical modelling study. *The Lancet Infectious Diseases* **20**, 1247–1254 (Nov. 2020).
14. Ilin, C., Annan-Phan, S., Tai, X. H., Mehra, S., Hsiang, S. & Blumenstock, J. E. Public mobility data enables COVID-19 forecasting and management at local and global scales. *Scientific Reports* **11**. ISSN: 2045-2322 (June 2021).
15. Mohammadi, Z., Cojocaru, M. G. & Thommes, E. W. Human behaviour, NPI and mobility reduction effects on COVID-19 transmission in different countries of the world. *BMC Public Health* **22** (Aug. 2022).
16. Xiong, C., Hu, S., Yang, M., Luo, W. & Zhang, L. Mobile device data reveal the dynamics in a positive relationship between human mobility and COVID-19 infections. *Proceedings of the National Academy of Sciences* **117**, 27087–27089 (Oct. 2020).
17. Harris, J. E. Mobility was a significant determinant of reported COVID-19 incidence during the Omicron Surge in the most populous U.S. Counties. *BMC Infectious Diseases* **22** (Aug. 2022).
18. Jewell, S., Futoma, J., Hannah, L., Miller, A. C., Foti, N. J. & Fox, E. B. It’s complicated: characterizing the time-varying relationship between cell phone mobility and COVID-19 spread in the US. *npj Digital Medicine* **4** (Oct. 2021).
19. Nanda, R. O., Nursetyo, A. A., Ramadona, A. L., Imron, M. A., Fuad, A., Setyawan, A. & Ahmad, R. A. Community Mobility and COVID-19 Dynamics in Jakarta, Indonesia. *International Journal of Environmental Research and Public Health* **19**. ISSN: 1660-4601 (2022).
20. Müller, S. A., Balmer, M., Charlton, W., Ewert, R., Neumann, A., Rakow, C., Schlenther, T. & Nagel, K. Predicting the effects of COVID-19 related interventions in urban settings by combining activity-based modelling, agent-based simulation, and mobile phone data. *PLOS ONE* **16** (ed Benenson, I.) (Oct. 2021).
21. Vecherin, S., Chang, D., Wells, E., Trump, B., Meyer, A., Desmond, J., Dunn, K., Kitsak, M. & Linkov, I. Assessment of the COVID-19 infection risk at a workplace through stochastic microexposure modeling. *Journal of Exposure Science & Environmental Epidemiology* **32**, 712–719 (Jan. 2022).
22. Liu, X., Huang, J., Li, C., Zhao, Y., Wang, D., Huang, Z. & Yang, K. The role of seasonality in the spread of COVID-19 pandemic. *Environmental Research* **195**, 110874. ISSN: 0013-9351 (2021).
23. Xu, R., Rahmandad, H., Gupta, M., DiGennaro, C., Ghaffarzagdegan, N., Amini, H. & Jalali, M. The Modest Impact of Weather and Air Pollution on COVID-19 Transmission (2020).
24. Hartmann, A., Cetin, Y. E., Gastmeier, P. & Kriegel, M. Practical application of CO<sub>2</sub> as an indicator regarding the risk of infection (July 2022).

25. Nordrhein-Westfalen, S. *Nordrhein-Westfalen-Plan tritt in Kraft / Stufenweise Öffnung der Anti-Corona-Maßnahmen startet in der kommenden Woche* <https://www.land.nrw/pressemitteilung/nordrhein-westfalen-plan-tritt-kraft-stufenweise-oeffnung-der-anti-corona>. [Accessed 10-01-2024]. 2020.
26. Mundt, M., Mathisen, H., Moser, M. & Nielsen, P. *Ventilation Effectiveness: Rehva Guidebooks* English. *Rehva Guidebook 2*. ISBN: (ISBN-10) 2960046803 (Federation of European Heating and Ventilation Association, 2004).
27. Kriegel, M. & Hartmann, A. SARS-CoV-2-Aerosolpartikel: Inhalierete Dosen im Vergleich zwischen gar nicht, mäßig, gut und sehr gut belüfteten Räumen, 3–7 (2021).
28. Cori, A., Ferguson, N., Fraser, C. & Cauchemez, S. A New Framework and Software to Estimate Time-Varying Reproduction Numbers During Epidemics. *Am. J. Epidemiol.* (2013).
29. An der Heiden, M. *SARS-CoV-2-Nowcasting und -R-Schaetzung* June 2023.
30. Billah, M. A., Miah, M. M. & Khan, M. N. Reproductive number of coronavirus: A systematic review and meta-analysis based on global level evidence. *PLOS ONE* **15** (ed Flacco, M. E.) e0242128. ISSN: 1932-6203 (Nov. 2020).
31. WHO. *Statement on the meeting of the International Health Regulations (2005) Emergency Committee regarding the outbreak of novel coronavirus 2019 (n-CoV) on 23 January 2020 — who.int* [https://www.who.int/news/item/23-01-2020-statement-on-the-meeting-of-the-international-health-regulations-\(2005\)-emergency-committee-regarding-the-outbreak-of-novel-coronavirus-\(2019-ncov\)](https://www.who.int/news/item/23-01-2020-statement-on-the-meeting-of-the-international-health-regulations-(2005)-emergency-committee-regarding-the-outbreak-of-novel-coronavirus-(2019-ncov)). [Accessed 17-11-2023]. 2020.
32. Prada, J. P., Maag, L. E., Siegmund, L., Bencurova, E., Liang, C., Koutsilieri, E., Dandekar, T. & Scheller, C. Author Correction: Estimation of R0 for the spread of SARS-CoV-2 in Germany from excess mortality. *Scientific Reports* **12**. ISSN: 2045-2322 (Dec. 2022).
33. Böttcher, S., Oh, D.-Y., Staat, D., Stern, D., Albrecht, S., Wilrich, N., Zacher, B., Mielke, M., Rexroth, U., Hamouda, O. & Seifried, J. *Erfassung der SARS-CoV-2-Testzahlen in Deutschland (Stand 2.12.2020)* 2020.
34. Google LLC. *Google COVID-19 Community Mobility Reports* <https://www.google.com/covid19/mobility/>. 2022.
35. Bundesregierung. *Telefonkonferenz der Bundeskanzlerin mit den Regierungschefinnen und Regierungschefs der Länder am 13. Dezember 2020* <https://www.bundesregierung.de/resource/blob/997532/1827366/69441fb68435a7199b3d3a89bff2c0e6/2020-12-13-beschluss-mpk-data.pdf?download=1>. [Accessed 18-11-2023]. 2020.
36. Robert Koch-Institut. *7-Tage-Inzidenz der COVID-19-Fälle in Deutschland* Feb. 2024.
37. Schilling, J., Buda, S., Fischer, M., Goerlitz, L., Grote, U., Haas, W., Hamouda, O., Prahm, K. & Tolksdorf, K. Retrospektive Phaseneinteilung der COVID-19-Pandemie in Deutschland bis Februar 2021, 3–12 (2021).
38. Bundesregierung. *Telefonschaltkonferenz der Bundeskanzlerin mit den Regierungschefinnen und Regierungschefs der Länder am 30. April 2020* <https://www.bundesregierung.de/resource/blob/975226/1749804/5a0bd6bd8cf1af27f15b1498e379c592/2020-04-30-beschluss-bund-laender-data.pdf?download=1>. 2020.
39. Ganyani, T., Kremer, C., Chen, D., Torneri, A., Faes, C., Wallinga, J. & Hens, N. Estimating the generation interval for coronavirus disease (COVID-19) based on symptom onset data, March 2020. *Eurosurveillance* **25**. ISSN: 1560-7917 (Apr. 2020).
40. Xu, X., Wu, Y., Kummer, A. G., Zhao, Y., Hu, Z., Wang, Y., Liu, H., Ajelli, M. & Yu, H. Assessing changes in incubation period, serial interval, and generation time of SARS-CoV-2 variants of concern: a systematic review and meta-analysis. *BMC Medicine* **21**. ISSN: 1741-7015 (Sept. 2023).
41. Hart, W. S., Miller, E., Andrews, N. J., Waight, P., Maini, P. K., Funk, S. & Thompson, R. N. Generation time of the alpha and delta SARS-CoV-2 variants: an epidemiological analysis. *The Lancet Infectious Diseases* **22**, 603–610. ISSN: 1473-3099 (May 2022).
42. Apple. *COVID-19 mobility trends reports* 2020.
43. Meteostat. *Meteostat Bulk Data* <https://dev.meteostat.net/bulk/>. 2023.

44. Balmer, M., Ewert, R., Müller, S. A., Nagel, K., Neumann, A. & Rakow, C. *Episim mobility data on county level* version 1.0.0 (Zenodo, June 2022).
45. Schlosser, F., Maier, B. F., Jack, O., Hinrichs, D., Zachariae, A. & Brockmann, D. COVID-19 lockdown induces disease-mitigating structural changes in mobility networks. *Proceedings of the National Academy of Sciences* **117**, 32883–32890 (Dec. 2020).
46. Jaekel, B. & Muley, D. Transport impacts in Germany and State of Qatar: An assessment during the first wave of COVID-19. *Transportation Research Interdisciplinary Perspectives* **13**. ISSN: 2590-1982 (2022).
47. Walker, M. D. & Sulyok, M. The Relationship between Mobility and COVID-19 in Germany: Modeling Case Occurrence using Apple’s Mobility Trends Data. *Methods of Information in Medicine* **59**, 179–182 (Dec. 2020).
48. Anke, J., Francke, A., Schaefer, L.-M. & Petzoldt, T. Impact of SARS-CoV-2 on the mobility behaviour in Germany. *European Transport Research Review* **13** (Jan. 2021).
49. Ecke, L., Magdolen, M., Chlond, B. & Vortisch, P. Tracing the Effects of the Covid-19 Pandemic on Car Usage in Germany - an Analysis of the German Mobility Panel. en. *European Journal of Transport and Infrastructure Research* (2021).
50. König, A. & Dreßler, A. A mixed-methods analysis of mobility behavior changes in the COVID-19 era in a rural case study. *European Transport Research Review* **13** (Feb. 2021).
51. Ehlert, A. & Wedemeier, J. Which factors influence mobility change during COVID-19 in Germany? Evidence from German county data. *Regional Science Policy & Practice* **14**, 61–79 (May 2022).
52. Bönisch, S., Wegscheider, K., Krause, L., Sehner, S., Wiegel, S., Zapf, A., Moser, S. & Becher, H. Effects of Coronavirus Disease (COVID-19) Related Contact Restrictions in Germany, March to May 2020, on the Mobility and Relation to Infection Patterns. *Frontiers in Public Health* **8** (Oct. 2020).
53. Becher, H., Bönisch, S. & Wegscheider, K. Reduction of Mobility During the COVID-19 Pandemic in Germany According to Age, Sex, and Federal State. *Deutsches Ärzteblatt international* (Aug. 2021).
54. Brasche, S. & Bischof, W. Daily time spent indoors in German homes – Baseline data for the assessment of indoor exposure of German occupants. *International Journal of Hygiene and Environmental Health* **208**, 247–253 (July 2005).

## **Author contribution**

- Conceptualization: SP, KN
- Data curation: SP
- Formal analysis: SP
- Investigation: SP
- Methodology: SP, IB, KN
- Visualization: SP
- Writing - original draft : SP, KN
- Writing - review and editing: SP, IB, KN
- Funding acquisition: KN
- Project administration: SP, KN
- Supervision: KN

## **Acknowledgements**

The work on the paper was in part funded by the Ministry of research and education (BMBF) Germany (grants number 031L0300D, 031L0302A, 031L0302C), and by TU Berlin. The BMBF Grant also funded the data provided by the commercial company Senozon.

## **Additional Information**

**Declaration of interests:** The authors declare no competing interests.

## 5 Supplementary material

### 5.1 Relationship of COVID-19 and mobility in Germany

As noted in Section 1.2.1, multiple studies investigate the reduction of mobility in Germany related to the COVID-19 pandemic:

Conducting an analysis of movement records from mobile phones, [45] found that lockdown measures caused substantial and long-lasting structural changes in mobility, noting a heterogeneous spatial distribution of reductions (increased reduction in large cities compared to less densely populated areas) and the largest reduction for mid-March 2020. By analyzing the Google mobility data [34] for the federal state of Saxony until July 2020, [46] found an overall decline in mobility for all commercial activities and an increase for parks and residential locations. Additionally, using the three mobility categories (transit, walking driving) of the Apple mobility data [42], [47] found a negative correlation between mobility and confirmed case numbers in Germany.

Using survey data from the first wave of the COVID-19 pandemic in Germany, [48] found the most significant mobility reduction for recreational trips followed by work trips. Here, public transit displays the largest decrease in share, in terms of modal split. [49] carried out a self-assessment survey, noting that the share of the adult population which had public transport in their mode choice set had dropped by almost half during the lockdown of spring 2020. Finally, concentrating on the rural population and using data from interviews and a survey, [50] found that a considerable share of respondents stated to not have changed their mobility behavior, and that in consequence insights from urban settings cannot be directly transferred to rural areas.

Returning to the question of mode choice, [49] investigated the car usage in Germany before (spring 2019) and during (spring 2020) the pandemic, finding an effect as overall mileage decreased (magnitude of decrease depended on household characteristic, age and cubic capacity of the car), but noting that at the time of writing it was unclear whether or not these changes will turn out to be structural.

Furthermore, [51] computed the change in general mobility behavior at the Germany county level in January 2021 compared to the same period of the previous year, finding that mobility changes show significant socioeconomic heterogeneity. Contrarily, analyzing continuous location (provided via a smartphone app, from beginning of March until mid-May 2020) in combination with demographic characteristics, [52] found that the German population reduced its mobility in a rather consistent and uniform way. They found no evidence for statistically significant period-by-subgroup interactions. In a follow-up research letter, [53] additionally analyzed the reduction in daily distance travelled by an individual person up until June 2021, again finding that the pattern of relative reduction was similar in all age groups and in both sexes, with a slightly higher relative mobility in the younger age group in summer 2020 and the last month of observation.

### 5.2 Comparison of mobility data sources

In this work, we have used the out-of-home duration by Senozon [44]. Alternative data sources are the Google COVID-19 Community Mobility Reports. The google mobility reports provide mobility data for six different categories, including “residential”. Mobility data is presented relative to a baseline value. For each day of the week, the baseline value is the median value from the 5-week period from January 3rd until February 6th, 2020. Assuming that an average person in Germany spends around 15.7 hours per day at home [54], the relative numbers for the category “residential” can be converted to absolute numbers, i.e. the amount of time people spent at home. From the absolute amount of time spent at home, one can then infer the amount of time people did not spend at home. This is then comparable to the number we have used above. Please note that when trying to apply our method to other nations, another assumption for the baseline out-of-home duration might be necessary.

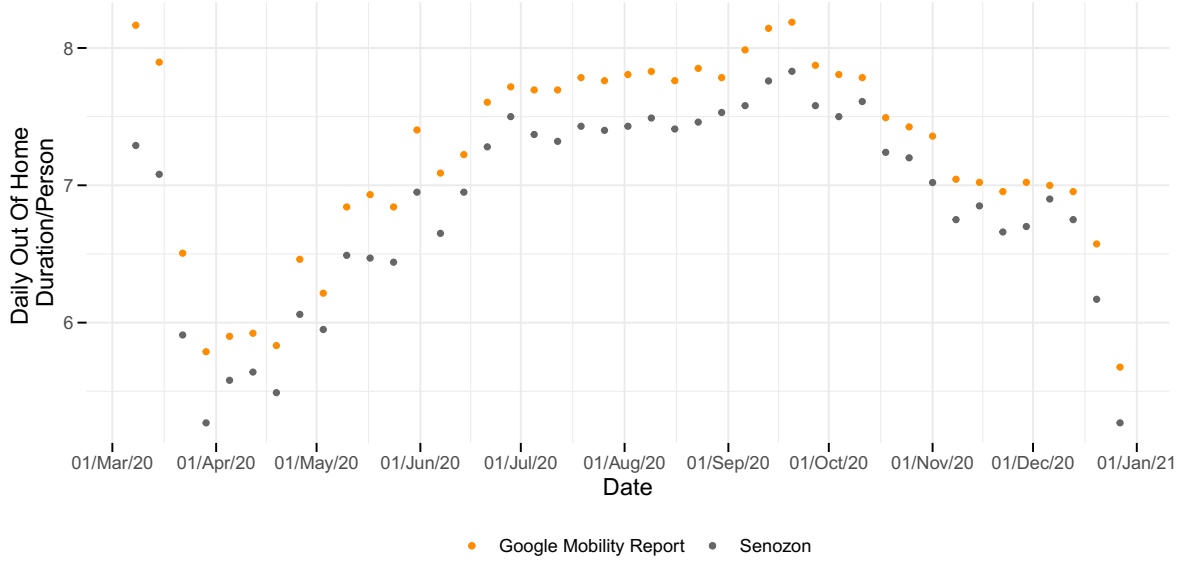


Figure 10: Daily out of home duration per person (in hours) for 2020. Comparison of Senozon and Google COVID-19 Community Mobility Reports data.

### 5.3 Model Comparison

#### Step 1 - Mobility only models

In a first step, we compare multiple mobility only models:

$$\mathbf{G}_{t+2} = \beta_0 + \beta_d \mathbf{D}_t^m.$$

Here, the growth multiplier is denoted by  $\mathbf{G}_t = I_{t+1}/I_t$ , where  $I_t$  is the weekly average incidence,  $t$  indexes the weeks, the out-of-home duration is denoted by  $\mathbf{D}_t$ , and for which  $m \in \{1, 2, 3\}$ . Based on the arguments detailed in Section 2.2, we decide on the quadratic model ( $m = 2$ ). For details and model outputs, see Section 2.2.

#### Step 2 - Intercept vs. no Intercept

In the second step, we compare the quadratic intercept and no-intercept model:

$$\begin{aligned} \mathbf{G}_{t+2} &= \beta_0 + \beta_d \mathbf{D}_t^2, \\ \mathbf{G}_{t+2} &= \beta_d \mathbf{D}_t^2, \end{aligned} \tag{17}$$

Again, the model outputs and our reasoning for continuing with the no-intercept model (17) are provided in Section 2.2.

#### Step 3 - Comparison of weather variables

As noted in Section 2.3, the inclusion of the share of activities performed outside (**outFrac**) instead of temperature itself, is based on our previous modelling work. To additionally support this variable transformation, we set up analogous models to (8), but with the weekly average of the daily maximum temperature **Tmax**, or the weekly average of the daily average temperature **Tavg** instead of **outFrac**. For **Tmax**, this model reads

$$\mathbf{G}_{t+2} = \beta_{d^2} \mathbf{D}_t^2 + \beta_{temp} \mathbf{Tmax}_t + \beta_{tempd^2} \mathbf{D}_t^2 \cdot \mathbf{Tmax}_t$$

and creates the output found in the following table:

Variable	Coefficient	Std. Error	$p >  t $	[95% CI]
$\mathbf{D}^2$	0.0268203	0.0019012	$< 2e - 16$	(0.0230, 0.0307)
$\mathbf{Tmax}$	-0.0067756	0.0095029	0.480	(-0.0260, 0.0125)
$\mathbf{D}^2 \cdot \mathbf{Tmax}$	-0.0001027	0.0001719	0.554	(-0.0005, 0.0002)
Adjusted $R^2$	0.5956			
AIC	-21.2415			
BIC	-14.48598			

Table 4: Model output, out-of-home duration  $\mathbf{D}$  and temperature  $\mathbf{Tmax}$  lead by 2.5 weeks.

Analogously, for  $\mathbf{Tavg}$  the corresponding model reads

$$\mathbf{G}_{t+2} = \beta_{d^2} \mathbf{D}_t^2 + \beta_{temp} \mathbf{Tavg}_t + \beta_{tempd^2} \mathbf{D}_t^2 \cdot \mathbf{Tavg}_t,$$

which leads to the output found in Table 5.

Variable	Coefficient	Std. Error	$p >  t $	[95% CI]
$\mathbf{D}^2$	$2.652e - 02$	$1.738e - 03$	$< 2e - 16$	(0.0230, 0.0300)
$\mathbf{Tavg}$	$-1.367e - 02$	$1.471e - 02$	0.359	(-0.0435, 0.0161)
$\mathbf{D}^2 \cdot \mathbf{Tavg}$	$-3.123e - 05$	$2.551e - 04$	0.903	(-0.0005, 0.0005)
Adjusted $R^2$	0.5992			
AIC	-21.59887			
BIC	-14.84335			

Table 5: Model output, out-of-home duration  $\mathbf{D}$  and temperature  $\mathbf{Tavg}$  lead by 2.5 weeks.

For comparison, the model for the outdoor fraction  $\mathbf{outFrac}$ , which we presented in Section 2.3, reads

$$\mathbf{G}_{t+2} = \beta_{d^2} \mathbf{D}_t^2 + \beta_o \mathbf{outFrac}_t + \beta_{od^2} \mathbf{D}_t^2 \cdot \mathbf{outFrac}_t. \quad (18)$$

and its result can be found in Table 6.

Variable	Coefficient	Std. Error	$p >  t $	[95% CI]
$\mathbf{D}^2$	0.0242	0.0008	$< 2e - 16$	(0.0226, 0.0259)
$\mathbf{outFrac}$	0.0167	0.3976	0.967	(-0.7889, 0.8222)
$\mathbf{D}^2 \cdot \mathbf{outFrac}$	-0.0053	0.0074	0.478	(-0.0204, 0.0097)
Adjusted $R^2$	0.6345			
AIC	-25.2865			
BIC	-18.5310			

Table 6: Model output of (18), out-of-home duration  $\mathbf{D}$  and outdoor fraction  $\mathbf{outFrac}$  lead by 2.5 weeks.

Besides temperature (and its transformation  $\mathbf{outFrac}$ ), it is possible that precipitation influences behavior and therefore, indirectly, the growth multiplier  $\mathbf{G}$ . We consider a model that includes the variable precipitation ( $\mathbf{Precip}$ ) and its interaction with the squared out-of-home duration  $\mathbf{D}^2$ . For  $\mathbf{Tmax}$ , this model reads

$$\mathbf{G}_{t+2} = \beta_{d^2} \mathbf{D}_t^2 + \beta_{temp} \mathbf{Tmax}_t + \beta_p \mathbf{Precip}_t + \beta_{tempd^2} \mathbf{D}_t^2 \cdot \mathbf{Tmax}_t + \beta_{pd^2} \mathbf{D}_t^2 \cdot \mathbf{Precip}_t$$

and produces the model output found in Table 7.

Variable	Coefficient	Std. Error	$p >  t $	[95% CI]
$\mathbf{D}^2$	0.0266581	0.0020713	$7.84e - 15$	(0.0224532100, 0.0308630041)
$\mathbf{Tmax}$	0.0009636	0.0116898	0.935	(-0.0227679034, 0.0246950782)
$\mathbf{Precip}$	-0.1612546	0.1498053	0.289	(-0.4653755335, 0.1428662861)
$\mathbf{D}^2 \cdot \mathbf{Tmax}$	-0.0002581	0.0002195	0.248	(-0.0007037921, 0.0001874938)
$\mathbf{D}^2 \cdot \mathbf{Precip}$	0.0032761	0.0028741	0.262	(-0.0025586248, 0.0091107965)
Adjusted $R^2$	0.6111			
AIC	-18.80341			
BIC	-8.670129			

Table 7: Model output, out-of-home duration  $\mathbf{D}$ , temperature  $\mathbf{Tmax}$ , and precipitation  $\mathbf{Precip}$  lead by 2.5 weeks.

For  $\mathbf{Tavg}$ , the corresponding model reads

$$\mathbf{G}_{t+2} = \beta_{d^2} \mathbf{D}_t^2 + \beta_{temp} \mathbf{Tavg}_t + \beta_p \mathbf{Precip} + \beta_{tempd^2} \mathbf{D}_t^2 \cdot \mathbf{Tavg}_t + \beta_{pd^2} \mathbf{D}_t^2 \cdot \mathbf{Precip}_t$$

with the output found in Table 8.

Variable	Coefficient	Std. Error	$p >  t $	[95% CI]
$\mathbf{D}^2$	0.0262721	0.0018416	$3.75e - 16$	(0.022533560, 0.0300106975)
$\mathbf{Tavg}$	-0.0014775	0.0181616	0.936	(-0.038347507, 0.0353925863)
$\mathbf{Precip}$	-0.1631482	0.1524124	0.292	(-0.472561924, 0.1462654806)
$\mathbf{D}^2 \cdot \mathbf{Tavg}$	-0.0002820	0.0003317	0.401	(-0.000955435, 0.0003914227)
$\mathbf{D}^2 \cdot \mathbf{Precip}$	0.0034440	0.0029206	0.246	(-0.002485039, 0.0093730891)
Adjusted $R^2$	0.6184			
AIC	-19.5587			
BIC	-9.425426			

Table 8: Model output, out-of-home duration  $\mathbf{D}$ , temperature  $\mathbf{Tavg}$ , and precipitation  $\mathbf{Precip}$  lead by 2.5 weeks.

Finally, for the outdoor fraction  $\mathbf{outFrac}$ , the model reads

$$\mathbf{G}_{t+2} = \beta_{d^2} \mathbf{D}_t^2 + \beta_o \mathbf{outFrac}_t + \beta_p \mathbf{Precip} + \beta_{od^2} \mathbf{D}_t^2 \cdot \mathbf{outFrac}_t + \beta_{pd^2} \mathbf{D}_t^2 \cdot \mathbf{Precip}_t \quad (19)$$

and its output can be found in Table 9.

Variable	Coefficient	Std. Error	$p >  t $	[95% CI]
$\mathbf{D}^2$	0.024256	0.001133	$< 2e - 16$	(0.021955690, 0.026555956)
<b>outFrac</b>	0.201940	0.426215	0.639	(-0.663322464, 1.067201797)
<b>Precip</b>	-0.149454	0.122266	0.230	(-0.397667222, 0.098759067)
$\mathbf{D}^2 \cdot \mathbf{outFrac}$	-0.009031	0.008045	0.269	(-0.025363158, 0.007300653)
$\mathbf{D}^2 \cdot \mathbf{Precip}$	0.002909	0.002319	0.218	(-0.001799981, 0.007616995)
Adjusted $R^2$	0.6502			
AIC	-23.05226			
BIC	-12.91899			

Table 9: Model output, out-of-home duration  $\mathbf{D}$ , outdoor fraction **outFrac**, and precipitation **Precip** lead by 2.5 weeks.

We note that model (19) has the highest adjusted  $R^2$  (0.6502), directly followed by model (18) (0.6345). However, for model (18), both AIC and BIC display lower values. Consequently, we decide to continue with model (18).

#### Step 4 - Only considering weather in combination with mobility

In Section 2.3, we highlighted statistically and theoretically motivated reasons for excluding the linear term **outFrac** (see Section 2.3 for details). The model from the aforementioned section was

$$\mathbf{G}_{t+2} = \beta_{d^2} \mathbf{D}_t^2 + \beta_{od^2} \mathbf{D}_t^2 \cdot \mathbf{outFrac}_t$$

and had the output shown in Table 10.

Variable	Coefficient	Std. Error	$p >  t $	[95% CI]
$\mathbf{D}^2$	0.0242	0.0008	$< 2e - 16$	(0.0226, 0.0258)
$\mathbf{D}^2 \cdot \mathbf{outFrac}$	-0.0050	0.0015	0.0017	(-0.0081, -0.0020)
Adjusted $R^2$	0.6345			
AIC	-27.2846			
BIC	-22.2180			

Table 10: Model output for final model, out-of-home duration  $\mathbf{D}$  and outdoor fraction **outFrac** lead by 2.5 weeks.

## 5.4 Model selection via Best subset selection, Lasso regularization, elastic net regularization

In Section 2.2 (and in Supplementary material 5.3), theoretical assumptions as well as visual results (see 1) guided the model selection. Complementary, in this subsection we show that using three different variable selection methods, namely best subset selection, Lasso regularization, and elastic net regularization, supports our conclusion.

Due to the arguments presented in Section 2.2, we consider the mobility variable  $\mathbf{D}$  up the degree three, the outdoor fraction **outFrac** up to degree three and every combination of them up until degree 3, leaving us with 9 predictors ( $\mathbf{D}$ ,  $\mathbf{D}^2$ ,  $\mathbf{D}^3$ , **outFrac**, **outFrac**<sup>2</sup>, **outFrac**<sup>3</sup>,  $\mathbf{D} \times \mathbf{outFrac}$ ,  $\mathbf{D}^2 \times \mathbf{outFrac}$ ,  $\mathbf{D} \times \mathbf{outFrac}^2$ ), and  $2^9$  models to choose from. Furthermore, due to the reasoning presented in Section 2.2, we enforce that the intercept is equal to 0.

### 5.4.1 Best subset selection

Best subset selection aims to find a small subset of predictors for a linear model. When performing best subset selection, a separate least squares regression model must be fit for each possible combination the predictor variables. For every possible subset size of variables, the best subset selection chooses the model with the minimal residual sum of squares (RSS). A single best model can then chosen by using one of the following three statistics: Bayesian Information Criterion (BIC), Mallor's  $C_p$  or adjusted  $R^2$ . Here, we consider all three of them, to choose a model which best satisfies our needs. In addition, we enforce that the maximum number of independent variables is **3**.

**BIC:** Comparing the  $2^9$  possible models, the model with the smallest BIC is

$$\mathbf{G}_{t+2} = \beta_{d^2} \mathbf{D}^2 + \beta_{d^2 o} \mathbf{D}^2 \cdot \text{outFrac}.$$

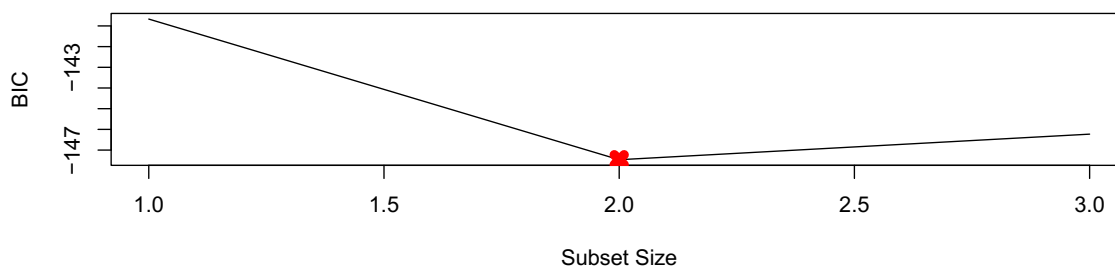


Figure 11: BIC for the different subset sizes.

**Mallow's  $C_p$ :** Among all models, the model with the smallest  $C_p$  is the following one:

$$\mathbf{G}_{t+2} = \beta_{d^3} \mathbf{D}^3 + \beta_{do} \mathbf{D} \cdot \text{outFrac} + \beta_{d^2 o} \mathbf{D}^2 \cdot \text{outFrac}$$

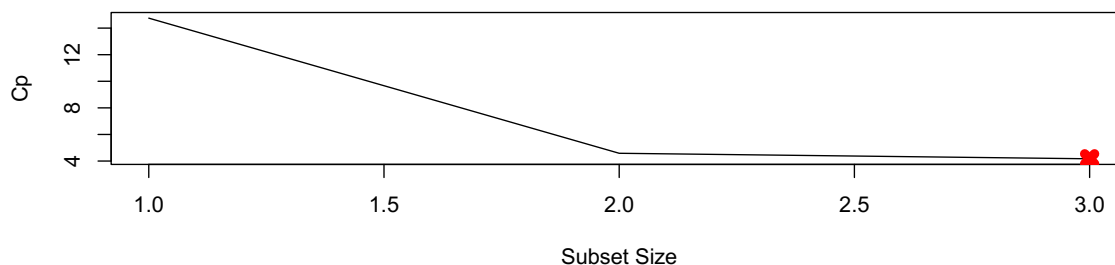


Figure 12: Mallor's  $C_p$  for the different subset sizes.

**Adjusted  $R^2$ :** And finally, among all  $2^9$ , the model with the largest adjusted  $R^2$  is as follows:

$$\mathbf{G}_{t+2} = \beta_{d^3} \mathbf{D}^3 + \beta_{do} \mathbf{D} \cdot \text{outFrac} + \beta_{d^2 o} \mathbf{D}^2 \cdot \text{outFrac}$$

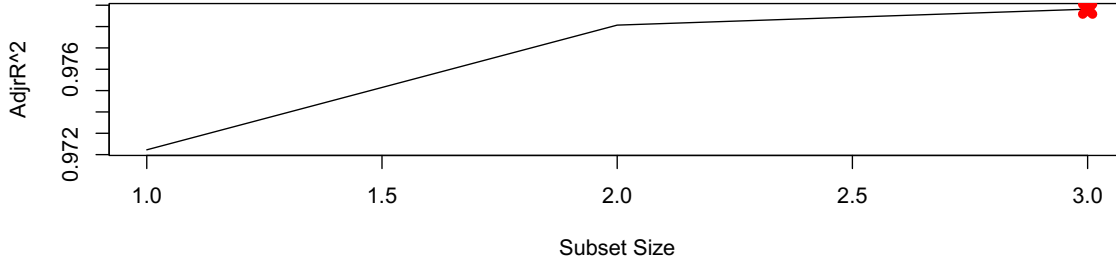


Figure 13: Adjusted  $R^2$  for the different subset sizes. The maximal adjusted  $R^2$  is equal to 0.6562 and reached, when the subset size is equal to 3. However, already when the subset size is equal to 2, we obtain an adjusted  $R^2$  of 0.6345.

#### 5.4.2 Lasso regularization

Lasso is a regression method which performs both variable selection and regularization with the aim of improving interpretability and model accuracy. In our case, Lasso regularization favors the model

$$\mathbf{G}_{t+2} = \beta_d \mathbf{D} + \beta_{d^2} \mathbf{D}^2 + \beta_{d^3} \mathbf{D}^3 + \beta_{o^3} \mathbf{outFrac}^3 + \beta_{d^2 o} \mathbf{D}^2 \cdot \mathbf{outFrac}$$

#### 5.4.3 Elastic net regularization

Elastic net regularization is a penalized linear regression model combining both  $L_1$  and  $L_2$  penalties. In consequence, elastic net regularization can be viewed as a combination of Ridge and Lasso regression. As the degree of mixing  $\alpha$  we chose  $\alpha = 0.5$  and chose the shrinkage parameter using 10-fold cross validation. The cross validation was performed 100 times, giving us a distribution of  $\lambda$ s. Both  $\text{mean}(\lambda)$  and  $\text{median}(\lambda)$  favor the model

$$\mathbf{G}_{t+2} = \beta_d \mathbf{D} + \beta_{d^2} \mathbf{D}^2 + \beta_{d^3} \mathbf{D}^3 + \beta_{o^3} \mathbf{outFrac}^3 + \beta_{d^2 o} \mathbf{D}^2 \cdot \mathbf{outFrac}$$

#### 5.4.4 Conclusion

Summarizing the results of the best subset selection, the lasso regularization and the elastic net regularization above, we observe that the different variable selection methods favor different models. However, we note that all three methods (as well as the 3 different criteria when applying best subset selection) select  $\mathbf{D}^2 \times \mathbf{outFrac}$  as an independent variable and lasso regularization, elastic net regularization as well as BIC (when applying best subset selection) also include  $\mathbf{D}^2$ . Contrarily, Mallor's  $C_p$  and the adjusted  $R^2$  favor  $\mathbf{D}^3$  as the mobility-only variable. Furthermore, when deciding based on BIC in best subset selection, the model  $\mathbf{G}_{t+2} = \beta_{d^3} \mathbf{D}^3 + \beta_{d^2 o} \mathbf{D}^2 \times \mathbf{outFrac}$  is chosen, which is the model we have already favored in Section 2.3. By Occam's razor, and as best subset selection is the preferable method in this case, we decide on  $\mathbf{G}_{t+2} = \beta_{d^2} \mathbf{D}^2 + \beta_{d^2 o} \mathbf{D}^2 \times \mathbf{outFrac}$  as the final model.

### 5.5 Model diagnostics

In order to assess the adequacy of the final Model (9), several model diagnostics were conducted. Figure 14 presents a scatter plot of the residuals against the predicted values from the model (top) as well as a scatter plot of the square root of the absolute value of the standardized residuals against the predicted values from the model (bottom). According to the assumption of homoscedasticity, we expect both panels to exhibit a random scatter of points around zero. However, the rightmost portion of the top panel suggests the presence of heteroscedasticity and a potential non-linear relationship. To further investigate this, a Breusch-Pagan test was performed, which examines the presence of heteroscedasticity in the residuals. The test yields a p-value of 0.1479 ( $> 0.05$ ), indicating a lack of evidence for heteroscedasticity.

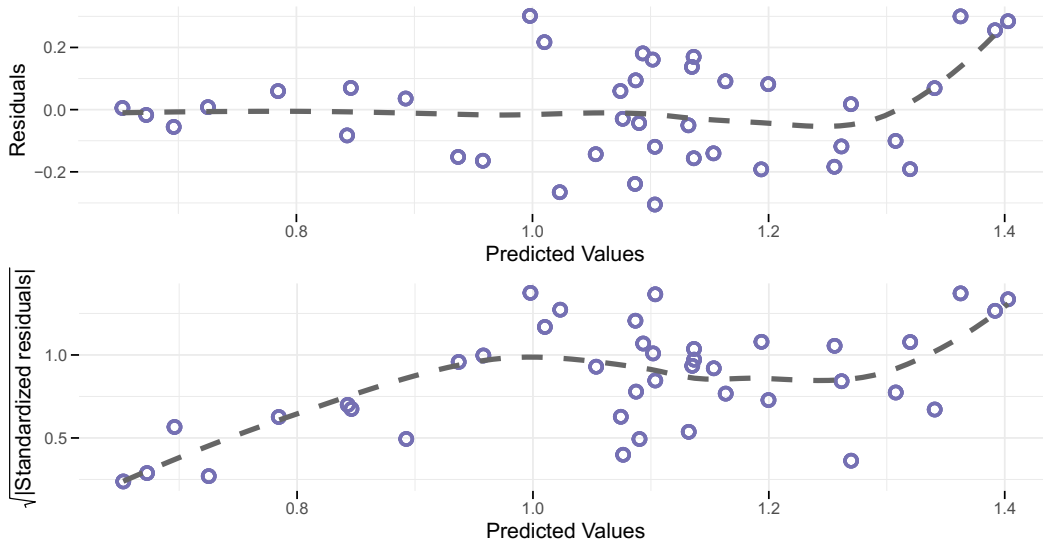


Figure 14: Top: Residuals vs. predicted values, bottom:  $\sqrt{|\text{Standardized residuals}|}$  vs. predicted values.

Figure 15 (top) shows the model residual quantiles vs. the theoretical quantiles if the residuals were to follow a normal distribution. A slight deviation can be noticed at the extreme ends, while the vast majority of the model quantiles aligns well with the theoretical quantiles. Finally, we use Cook's distance to detect observations that strongly influence fitted values of the model, which can be seen in Figure 15. Observations with a Cook's distance larger than the threshold of  $4/n$ , where  $n$  is the number of observations, are traditionally deemed outliers. With  $n = 40$ , three observations pass this threshold: Observation number 33 (corresponding to 18-October-2020) displays the largest Cook's distance ( $1.436696e - 01$ ), observation 34 (corresponding to 25-October-2020) displays the second largest Cook's distance ( $1.381654e - 01$ ), and observation 32 (corresponding to 11-October-2020) displays the third-largest cook's distance ( $1.092919e - 01$ ).

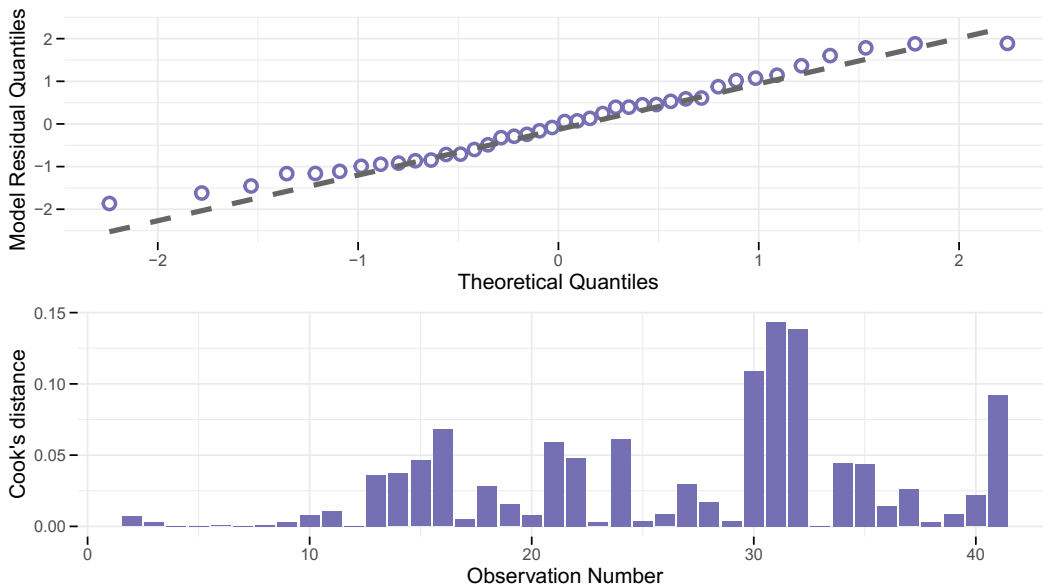


Figure 15: Top: Normal Q-Q plot, bottom: Bar plot of Cook's distance.

Altogether, the model diagnostics as well as Figure 3a and Figure 3b indicate that the model generally seems appropriate for the relationship that we aim to model, but three outliers at the beginning of the second wave are not fully explained by the proposed model, which were discussed elaborately in Section 3.